Aberrant association of chromatin with nuclear periphery induced by Rif1 leads to mitotic defect

Yutaka Kanoh[1], Seiji Matsumoto[1], Masaru Ueno[2], Motoshi Hayano[3], Satomi Kudo[1] and Hisao Masai[1]*

[1] Department of Basic Medical Sciences, Tokyo Metropolitan Institute of Medical Science, Setagaya-ku, Tokyo, Japan; [2] Graduate School of Integrated Sciences for Life, Hiroshima University, 1-3-1 Kagamiyama, Higashi-Hiroshima 739-8530, Japan; [3] Department of Neuropsychiatry, Keio University, 35 Shinano-machi, Shinjuku-ku, Tokyo, Japan

*Correspondence should be addressed to
Hisao Masai
Tel: +81-3-5316-3220; Fax: 03-5316-3145; E-mail: masai-hs@igakuken.or.jp

Summary Blurb

Overexpression of Rif1 induces relocation of chromatin to nuclear periphery and mitotic defect, suggesting a role of regulated chromatin-nuclear membrane association in proper progression of M phase.

Abstract

Architecture and nuclear location of chromosomes affect chromatin events. Rif1, a crucial regulator of replication timing, recognizes G-quadruplex and inhibits origin firing over the 50~100-kb segment in fission yeast, *Schizosaccharomyces pombe*, leading us to postulate that Rif1 may generate chromatin higher-order structures inhibitory for initiation. However, effects of Rif1 on chromatin localization in nuclei have not been known. We show here that Rif1 overexpression causes growth inhibition and eventually cell death in fission yeast. Chromatin binding activity of Rif1, but not recruitment of phosphatase PP1, is required for growth inhibition. Overexpression of a PP1-binding-site mutant of Rif1 does not delay S-phase, but still causes cell death, indicating that cell death is caused not by S-phase problems but by issues in other phases of cell cycle, most likely M-phase. Indeed, Rif1 overexpression generates cells with unequally segregated chromosomes. Rif1 overexpression relocates chromatin near nuclear periphery in a manner dependent on its chromatin-binding ability, and this correlates with growth inhibition. Thus, coordinated progression of S- and M-phases may require regulated Rif1-mediated chromatin association with nuclear periphery

Introduction

Chromosomes are packaged and compartmentalized in nuclei in an organized manner and their spatial arrangement and regional interactions regulate various chromosome transactions. Presence of chromosome near nuclear periphery is generally associated with inactive transcription or late replication (Lemaitre & Bickmore, 2015; Mahamid *et al*, 2016). The nuclear lamina, nuclear pore complexes and epigenetic regulators have been implicated in regulating tethering of chromatin at nuclear periphery (Amiad-Pavlov *et al*, 2021; Arib & Akhtar, 2011; Laghmach *et al*, 2021; Ptak & Wozniak, 2016; See *et al*, 2020; Smith *et al*, 2021). Rif1 was identified as a regulator of replication timing and was shown to suppress late origin firing. On the basis of effect of a Rif1 binding site mutant on origin firing patterns and biochemical functions of Rif1 protein, we have proposed that Rif1 regulates replication timing partly through generating specific chromatin architecture in fission yeast, *Schizosaccharomyces pombe* (Kanoh *et al*, 2015; Kobayashi *et al*, 2019; Masai *et al*, 2019). In mammalian cells, Rif1 is localized near nuclear periphery and was shown to regulate chromatin loop formation (Cornacchia *et al*, 2012; Foti *et al*, 2016; Yamazaki *et al.*, 2012). However, how Rif1 regulates chromatin localization and its potential roles in regulation of cellular events have not been well known. We have tested this by examining the effects of overexpression of Rif1 on the cell cycle progression and chromatin states in fission yeast cells.

Rif1, originally isolated as a telomere binding factor, is a multifunctional protein that regulates various aspects of chromosome dynamics, including DSB repair, DNA replication, recombination, transcription and others (Campolo *et al*, 2013; Cornacchia *et al.*, 2012; Di Virgilio *et al*, 2013; Hayano *et al*, 2012; Klein *et al*, 2021; Yamazaki *et al.*, 2012; Yoshizawa-Sugata *et al*, 2021; Zimmermann *et al*, 2013). Fission yeast Rif1 binds to chromatin, most notably at the telomere and telomeres are elongated in *rif1*Δ cells (Kanoh & Ishikawa, 2001; Kobayashi *et al.*, 2019). Hayano *et al*. reported that *rif1*Δ can restore the growth of *hsk1*Δ cells (Hayano *et al.*, 2012), indicating that the loss of *rif1* can bypass the requirement for the fission yeast "Cdc7" kinase (Dbf4-dependent kinase; DDK), which is essential for replication initiation under normal growth conditions. Late-firing origins are extensively deregulated in *rif1*Δ cells, consistent with a role for Rif1 in suppressing late-firing origins. Similarly, mammalian

Rif1 was also found to regulate the genome-wide replication timing (Cornacchia *et al.*, 2012; Klein *et al.*, 2021; Yamazaki *et al.*, 2012). Rif1 interacts with PP1 phosphatase through its PP1 binding motifs, and the recruitment of the phosphatase by Rif1 counteracts the phosphorylation events that are essential for initiation of DNA replication including the phosphorylation of Mcm, explaining a mechanism of Rif1-mediated inhibition of replication initiation (Dave *et al*, 2014; Hiraga *et al*, 2014; Mattarocci *et al*, 2014; Shyian *et al*, 2016).

In addition to its binding to telomeres, fission yeast Rif1 also binds to the arm segments of the chromosomes. Thirty-five strong Rif1 binding sites (Rif1bs) have been identified on fission yeast chromosomes. These sequences contain multiple G-tracts and have propensity to form G-quadruplex (G4) structures (Kanoh *et al.*, 2015). Consistent with this, Rif1 specifically binds to G4-containing DNA *in vitro*, and mutations of G-tracts impaired both *in vivo* chromatin binding of Rif1 and *in vitro* interaction of Rif1 with the Rif1bs. Notably, loss of Rif1 binding at a single Rif1bs caused deregulation of late firing origins in the 50~100kb segment in its vicinity, consistent with the notion that Rif1 binding generates a chromosome compartment where origin firings are suppressed. In fission yeast, Rif1 was implicated also in resolution of non-telomeric ultrafine anaphase bridges (Zaaijer et al. 2016).

In mammals, Rif1 is preferentially localized at the nuclear periphery in the Triton X-100- and DNase I-resistant compartments, where it regulates the length of chromatin loops (Yamazaki *et al.*, 2012, 2013). In fission yeast, Rif1 is biochemically fractionated into Triton X-100- and DNase I-insoluble fractions (Kanoh *et al.*, 2015). In budding yeast, Rif1 was shown to be palmitoylated and the lipid modification-mediated membrane association plays important roles in DSB repair (Fontana *et al*, 2019; Park *et al*, 2011). However, it is unknown whether similar mechanisms operate for Rif1 from other species.

We hypothesized that Rif1 generates higher-order chromatin architecture through its ability to tether chromatin loops, and that this chromatin structure constitutes the replication inhibitory chromatin compartments that are deregulated during mid-S phase. In order to gain more insight into the roles of Rif1 in regulation of chromatin structure and cell cycle, we have analyzed the effect of Rif1 overexpression on the growth, cell cycle progression and chromatin structure in fission yeast, *Schizosaccharomyces pombe*. The results indicate that regulated association of

chromatin with nuclear periphery ,may play a crucial role in proper S- and M-phase progression.

Results

Overexpression of Rif1 prevents cell growth.

The *rif1* mutation was identified as a suppressor of the *hsk1-null* mutation (encoding Cdc7 kinase [DDK] homologue) in fission yeast, *Schizosaccharomyces pombe* (Hayano *et al.*, 2012) and we previously showed that Rif1 suppressed origin firing over ~100kb segments spanning its binding sites (Kanoh *et al.*, 2015). During the course of our experiments, we cloned the *rif1*$^{+}$ ORF into pREP41 and expressed Rif1 under the inducible nmt41 (No Message in Thiamine 1) promoter (**Fig 1A and B**). Induction of the full length Rif1 (1-1400aa) in medium without thiamine strongly inhibited growth of both *hsk1*$^{+}$ and *hsk1-89* (a temperature-sensitive stain) cells (**Fig 1C and D**). Various truncated deletion mutants of Rif1 were cloned and expressed from the inducible nmt41 promoter to examine growth in *hsk1*$^{+}$ or *hsk1-89* cells (**Fig 1B**). The expression levels of these truncation mutants were examined by western blotting and the results indicate that all the mutants are uniformly expressed (**Fig S1A**). We measured the numbers of Rif1 molecules in yeast cells. As a standard, we first purified His_6-Rif1(93-1400aa)-$Flag_3$, since we found that deletion of the N-terminal 92aa stabilized the protein (Moriyama et al. unpublished data). The amount of Rif1-$Flag_3$ expressed at the endogenous locus and on a plasmid was assessed by western blotting. The number of endogenous Rif1 molecule was estimated to be ~1,000, while that of plasmid-derived Rif1 was estimated to be 10,000 and 37,000 before and after induction, respectively (**Fig S1B**). A C-terminal 140-amino acids deletion (construct 1-1260aa) inhibited the growth of *hsk1*$^{+}$ weakly and *hsk1-89* strongly (**Fig 1C and D**). Further truncations of the Rif1 C-terminus (constructs 1-965aa and 1-442aa) result in complete loss of growth inhibition. We previously showed that truncation of the Rif1 C-terminal 140-amino acids (construct 1-1260aa) resulted in loss of telomere length regulation (Kobayashi *et al.*, 2019). Therefore, we conclude that the growth inhibition caused by overexpression of Rif1 does not depend on its function in telomere regulation. In contrast, deletion of the N-terminal 150-amino acids from Rif1 resulted in loss of growth inhibition (**Fig 1C and D**). However, deletion of the N-terminal 80-amino acids did not affect the ability of Rif1 to inhibit the growth in the *hsk1*$^{+}$ cells (**Fig 1C**), suggesting that the segment 81-150aa is important for inhibition. Taken together, the results suggest that the segment 81-1260aa may be required and sufficient for inhibition.

The N-terminal domain (88-1023aa) of fission yeast Rif1 is predicted to form a 3-D structure identical to that of the HEAT repeats by AlphaFold2 (Jumper *et al*, 2021). Thus, the HEAT domain 88-1023aa may play a major role for growth inhibition by Rif1, although it has not been experimentally tested if 88-1023aa is sufficient for inhibition.

Growth inhibition by Rif1-overexpression does not involve recruitment of PP1.

Rif1 recruits protein phosphatase 1 (PP1) through its PP1 binding motifs ($Rif1_{40-43}$ and $Rif1_{64-67}$) and the recruited PP1 counteracts the phosphorylation by Cdc7 kinase at origins (Dave *et al.*, 2014; Hiraga *et al.*, 2014; Mattarocci *et al.*, 2014). This interaction of Rif1 with PP1 is crucial for replication inhibition by Rif1 at late origins. Therefore, we examined whether Rif1-overexpression-induced growth inhibition is caused by hyper-recruitment of PP1. Fission yeast cells have two PP1 genes *dis2*$^+$ and *sds21*$^+$. A single disruption mutation of *dis2* or *sds21* is viable, but the double mutation is lethal (Kinoshita *et al*, 1990). *dis2-11* is a cold-sensitive mutant of *dis2*$^+$. We first examined whether growth inhibition caused by Rif1 overexpression depends on the PP1 genes. Overexpression of Rif1 in *dis2-11*, *dis2*Δ and *sds21*Δ resulted in strong growth inhibition in all the tested strains on EMM media without thiamine (**Fig 2A**). The extent of inhibition in each PP1 mutant was as strong as that observed in the wild-type, suggesting that the recruited PP1 is not responsible for the growth inhibition.

To further examine the involvement of PP1, we constructed a PP1-binding mutant of Rif1. We generated an alanine-substituted mutant of the two PP1 binding motifs (KVxF at aa40-43 and SILK at aa64-67) of Rif1 (**Fig 2B**) and confirmed, by immunoprecipitation, that the mutant Rif1 (PP1bsmut) did not bind to either Dis2 or Sds21 (**Fig 2C**; compare lanes14 and 17, lanes 15 and 18). Growth inhibition caused by overexpression of the PP1bsmut was comparable to or even slightly stronger than that caused by the wild-type Rif1 in both *rif1*$^+$ and *rif1*Δ backgrounds (**Fig 2D and E**). This is a further support for the conclusion that growth inhibition by Rif1-overexpression does not depend on recruitment of PP1. These results are consistent with the observation that the N-terminal truncation Rif1 (81-1400aa), which lacks the PP1 binding sites, can inhibit the growth upon overexpression (**Fig 1C**). As shown in the later section, the PP1bs mutant of Rif1 loses the ability to inhibit DNA synthesis, indicating that growth inhibition by Rif1 is related to the events other than S phase.

Growth inhibition by Rif1-overexpression does not depend on Taz1 or replication checkpoint.

We next asked whether the growth inhibition by overexpressed Rif1 is caused by counteracting the Hsk1-Dfp1/Him1 activity. Coexpression of both Hsk1 and Dfp1/Him1 under the control of the nmt1 promoter itself caused growth inhibition in fission yeast cells, and growth was partially restored by *rif1* deletion. However, overexpression of Hsk1-Dfp1/Him1 did not improve the growth of Rif1-overexpressing cells and inhibited the growth more strongly (**Fig S2A**), excluding the possibility that inhibition of growth is due to the reduced Hsk1 kinase actions. Consistent with the results of the C-terminal deletion mutant (1-1260aa), which does not interact with Taz1 but still inhibits growth (**Fig 1C and D**), mutation of *taz1*$^{+}$ known to be required for telomere-localization of Rif1 did not affect the growth inhibition by Rif1-overexpression (**Fig S2B**). Similarly, growth inhibition was observed in mutants of the replication checkpoint genes (Furuya & Carr, 2003), *rad3 tel1*, *rad3*, *chk1* or *cds1* (**Fig S2B**). The extent of growth inhibition was not affected by *cdc25-22* or *wee1-50*, genes involved in mitosis (Iino & Yamamoto, 1997; Kumar & Huberman, 2004; Rowley *et al*, 1992) (**Fig S2C**). These results suggest that the growth inhibition is not caused by replication or mitotic checkpoint functions or deregulation of mitotic kinases.

Effect of Rif1 overexpression on entry into S phase and replication checkpoint activation.

In order to clarify the mechanisms of Rif1-mediated growth inhibition, we examined whether Rif1 overexpression inhibits S phase initiation and progression. We synchronized cell cycle by release from *nda3*-mediated M phase arrest, and analyzed the DNA content by FACS. In the wild-type cells, DNA synthesis was observed at 30 min (at 18.5 hr in FACS chart in **Fig 3A**) from the release, and continued until 19.5 hr (90 min). In Pnmt41-Rif1, where Rif1 was overexpressed, DNA synthesis was delayed by 30 min (at 19.0 hr in FACS chart in **Fig 3A**) and was not completed even at 20 hr (120 min), indicating that Rif1 overexpression retarded the initiation and elongation of DNA synthesis. In contrast, in Pnmt41-*rif1*PP1bs mut, DNA synthesis occurred with timing similar to the wild-type, indicating that the overexpression of the PP1 mutant Rif1 does not affect the S phase (**Fig 3A and B**). This suggests that inhibition of S phase

by overexpressed Rif1 is due to the hyper-recruitment of PP1, which would counteract the phosphorylation events mediated by Cdc7 or Cdk and inhibit initiation.

We next examined whether overexpression of Rif1 activates replication checkpoint. We measured Cds1 kinase activity by in-gel kinase assay. While Cds1 kinase activity decreased at 12 hr after induction and then slightly increased afterward in cells overexpressing the wild-type Rif1, it continued to increase until 24 hr after overexpression of the PP1bs mutant (**Fig 3C and D**). These results indicate that overexpression of the *rif1*PP1bs mutant activates replication checkpoint, whereas the wild-type Rif1 does not, consistent with the above results that growth inhibition is not caused by replication checkpoint.

Short spindles and abnormally segregated nuclei are accumulated in cells overexpressing Rif1.

We next observed the morphological effects of Rif1-overexpression in cells expressing GFP-tagged histone H3 (*hht2+-GFP*) or GFP-tagged α-Tubulin (*GFP-α2tub*). Cells with aberrant morphology appeared in Rif1-overexpressing cells, indicative of failure of chromosome segregation. At 22 hr after induction, cells with abnormal nuclei accumulated and, notably, cells with unequally segregated nuclei reached ~30% of the cell population (**Fig 4A**). We then examined whether DNA damages are induced in these cells by measuring the cells with Rad52 foci, an indicator of DSB (Du *et al*, 2003; Matsumoto *et al*, 2005). Cells with nuclei containing Rad52 foci accumulated in Rif1-overexpressing cells (up to 44 % of the cells at 72 hr after induction; **Fig 4B**).

By using *GFP-α2tub* cells, we counted cells with spindle microtubules. In control cells (vector plasmid) and in the cells carrying pREP41-Rif1-$Flag_3$ grown with thiamine, most cells showed only cytoplasmic microtubules and roughly only 1% of cells showed spindle microtubules; either short or long spindles were detected in roughly 0.5% each of the cell population (**Fig 5A**). However, Rif1 overexpressing cells showed short spindles in up to 6% of the cell population and the population with long spindles decreased to one-half of the non-induced cells (**Fig 5A**). This result unexpectedly suggested that at least 5-6% of cells overexpressing Rif1 arrest mitosis in metaphase-anaphase transition. The above results suggest a possibility that spindle assembly checkpoint is induced by Rif1 overexpression. Therefore, we examined the effect of *mad2* and *bub1* (required for SAC [Spindle Assembly Checkpoint]) mutation

on the appearance of cells with spindles upon Rif1 overexpression (Bernard *et al*, 1998; Bernard *et al*, 2001; Garcia *et al*, 2001; Ikui *et al*, 2002). The population of the cells with short spindle microtubules decreased to 1% or less in *mad2*Δ and *bub1*Δ (**Fig 5B**), indicating that the formation of short spindles depends on SAC. We therefore examined whether SAC is induced by overexpression of Rif1. When SAC is activated, APC/Cdc20 ubiquitin ligase is inhibited. This would stabilize Securin (Cut2) and CyclinB. We then measured the effects of Rif1 overexpression on the duration of Cut2 signal together with the locations of Sad1 (spindle pole body). In the control cells, the spindle appeared at 4 min from division of Sad1 foci and disappeared by 12 min. The Cut2 signal disappeared at around 14 min. In contrast, in Rif1-overproducing cells, the spindle appearing at time 0 was still visible at 36-38 min. The Cut2 signal persisted even after 30 min (**Fig 5C**). These results show that SAC is activated by Rif1 overexpression. We then examined the effect of SAC mutations on the growth inhibition by Rif1-overexpression. Rif1 overexpression inhibited growth in *mad2*Δ and *bub1*Δ cells, indicating that growth inhibition is not caused by SAC (**Fig 5D**). It is of interest that Rif1 overexpression inhibited growth more vigorously in the SAC mutants than in the wild-type cells. Indeed, after Rif1 overexpression, cells with aberrant morphology increased from 4% in the wild-type cells to 8 % in *mad2*Δ and *bub1*Δ cells (**Fig 5E**). These results suggest that SAC activation may partially suppress the cell death-inducing effect of Rif1 overexpression.

The results indicate the aberrant chromatin segregation is responsible for growth inhibition and cell death. We noted that cells with aberrant spindles increased in cells overexpressing Rif1, and the fractions containing these structures were greater in PP1bs mutant overexpressing cells than in the wild-type Rif1 overexpressing cells (**Fig S3**). In contrast, the populations of the cells with short spindles decreased with PP1bs mutant compared to the wilt-type Rif1. This is due to decreased level of SAC activation in the cells overexpressing PP1bs mutant than in those overexpressing the wild-type Rif1.

Chromatin-binding of Rif1 is necessary for growth inhibition by Rif1 overexpression, and overexpressed Rif1 induces relocation of chromatin to nuclear periphery

We previously screened for *rif1* point mutants which suppress *hsk1-89*, and obtained two mutants, R236H and L848S, each of which alone could suppress *hsk1-89* (Kobayashi *et al.*, 2019). R236H bound to Rif1bs (Rif1bs$_{I:2663}$ and Rif1bs$_{II:4255}$) and to a telomere as efficiently as the wild type in ChIP assays. On the other hand, L848S did not bind to either of the two Rif1bs or to the telomere (Kobayashi *et al.*, 2019). We examined the effect of overexpression of these point mutants in wild-type and *hsk1-89* cells. R236H which can bind to chromatin caused growth defect in both wild type and *hsk1-89* when overexpressed (**Fig 6A**). On the other hand, L848S which is compromised in chromatin binding activity showed no or very little growth inhibition in the wild type. Interestingly, L848S inhibited the growth of *hsk1-89* (**Fig 6A**). Both mutant proteins were expressed at a level similar to that of the wild-type (data not shown).

The above results strongly suggest that chromatin binding of Rif1 is important for growth inhibition. Therefore, we have examined chromatin binding of overexpressed Rif1 protein by ChIP seq analyses. The results indicate that overexpressed Rif1 binds to multiple sites on the chromatin, in addition to its targets in the non-overproducing wild-type cells (**Fig 6B**). 128 peaks (Rif1 no OE) and 169 peaks (Rif1 OE) were identified by peak calling program MACS2 (listed in **Table 4** and **5)** and conserved sequence motifs were identified by MEME suites from the sequences of the Rif1 binding segments. Distribution of motif position probability was determined by STREME (provided from MEME suites) (**Fig 6C**). G-rich motifs were conserved and distributed around Rif1 binding segment in both "Rif1 no OE" and "Rif1OE". While there were two strong peaks on both sides of the Rif1BS summit with ~30 bp intervals in "Rif1 no OE", four peaks were detected in the 100 bp segment centering on the Rif1BS summit in "Rif1 OE", suggesting that Rif1 binding sequence specificity may be relaxed in Rif1 OE cells.

ChIP-qPCR showed that overexpressed Rif1 binds to known Rif1bs sequences as well as to a telomere with 3 to 7 fold higher efficiency than the endogenous Rif1 does, and binds also to a non-Rif1bs sequence (**Fig 6D**). There results suggest a possibility that the aberrant chromatin binding of Rif1 may be related to the induction of aberrant chromatin morphology and resulting growth inhibition and cell death.

We examined the chromatin morphology by using the cells containing GFP-labeled histone (h3.2-GFP). Interestingly, induction of Rif1 expression led to increased cell populations carrying nuclei with chromatin enriched at the nuclear periphery. This population reached over 6% with the wild type and 11 % with the rif1PP1BS mutant at 18 hr after induction (**Fig 7A and B**). Enrichment of chromatin at nuclear periphery could be caused by enlarged nucleoli as a result of Rif1 overproduction. We therefore measured the sizes of nucleoli by labeling Gar2 protein. We did not detect any effect on the sizes of nucleoli by overexpression of the wild-type or PP1bs mutant Rif1 protein (**Fig S4**), showing that chromatin relocation is not caused by enlarged nucleoli. The higher level of aberrant chromatin caused by the PP1bs mutant may be consistent with more severe growth inhibition with this mutant. The chromatin binding-deficient L848S mutant did not significantly induce relocation of chromatin, whereas R236H mutant, that is capable of chromatin binding, induced the relocation in 5% of the population (**Fig 7C and D**), in keeping with growth-inhibiting properties of the latter mutant but not of the former.

Nuclear dynamics of Rif1 protein

In order to visualize nuclear dynamics of Rif1 protein, we have fused a fluorescent protein to Rif1. Rif1 protein in higher eukaryotes contains a long IDP (intrinsically disordered polypeptide) segment between the N-terminal HEAT repeat sequences and C-terminal segment containing G4 binding and oligomerization activities. The fission yeast Rif1 does not carry IDP, but contains HEAT repeats and the C-terminal segment with similar biochemical activities. Thus, we speculated that insertion of a foreign polypeptide at the boundary of the two domains would least affect the overall structure of the protein, and introduced the mKO2 DNA fragment at aa1090/1091 or at aa1128/1129 (**Fig S5A**). The resulting plasmid DNAs were integrated at the endogenous *rif1* locus generating MIC11-130 *rif1*-mKO2-1 and MIC12-123 *rif1*-mKO2-2, respectively.

We then evaluated the functions of the fusion proteins. *hsk1-89* (ts) cells did not grow at 30°C (non-permissive temperature), whereas *hsk1-89 rif1*Δ cells did. On the other hand, *hsk1-89 rif1*-mKO2 did not grow at 30°C (**Fig S5B**), indicating that the Rif1-mKO2 retains the wild-type replication-inhibitory functions. In order to evaluate their telomere functions, we examined the telomere length in Rif1-mKO2 cells. As

reported, the telomere length increased in *rif1*Δ cells (**Fig S5C**, lane 2), whereas that in Rif1-mKO2-1 and -2 cells did not significantly change (**Fig S5C**, lanes 3 and 4), suggesting that the insertion of mKO2 does not affect the Rif1 function at telomeres. We chose Rif1-mKO2 (aa1090/1091) cells for further analysis. Rif1-mKO2 exhibited strong dots in nuclei (**Fig S5D and E**), which coloclalized with Taz1-GFP or Rap1-EGFP (**Fig S5D**, data not shown), indicating that they represent telomeres. Minute foci appeared in nuclei, probably representing Rif1 bound to the chromosome arms. Thus, Rif1-mKO2 (aa1090/1091) cells permit the visualization of dynamics of the endogenous Rif1 protein. Time laps analyses of Rif1-mKO2 revealed a few big foci in each cell which colocalize with Taz1 along with minute other nuclear foci that are highly dynamic and represent Rif1 on chromatin arms (**Supplementary movies; Fig S5D**).

Overexpression of Rif1 causes relocation of the endogenous Rif1 protein.

Upon overexpression of Rif1, either wild-type or a PP1bs mutant, in Rif1-mKO2 cells, mKO2 signals spread through nuclei (**Fig S5E**), consistent with the promiscuous chromatin binding of overexpressed Rif1. The overexpressed Rif1 would form mixed oligomers with the endogenous Rif1-mKO2, relocating some of the telomere-bound Rif1-mKO2 to chromosome arms. Prewash with 0.1% Triton X-100 and DNase I before PFA fixation led to appearance of multiple clear dots in nuclei in Rif1-mKO2 cells (**Fig 8A and Fig S6A**), since at least some of the Rif1 bound to chromatin arms is resistant to Triton/DNaseI pretreatment and that on telomere is more sensitive. Overexpression of Rif1 resulted in increased numbers of dots (**Fig 8A, B and Fig S6A, B, C**), consistent with the relocation of Rif1-mKO2 from the telomere to nuclear matrix-related insoluble compartments. The overall nuclear fluorescent intensities of the prewashed mKO2-Rif1 cells also increased after Rif1 overexpression compared to the vector control (**Fig 8C and Fig S6C**), consistent with above speculation. These results support the conclusion that overexpressed Rif1 promotes aberrant tethering of chromatin to nuclear membrane/ nuclear matrix-related insoluble compartments and that the resulting aberrant chromatin organization causes mitotic defect.

Discussion

Rif1 is an evolutionary conserved nuclear factor that plays roles in various chromosome transactions including DSB repair, DNA replication, transcription, and epigenetic regulation. Rif1 proteins from fission yeast and mammalian cells bind to G4 structure, and generate higher-order chromatin architecture (Kanoh *et al.*, 2015; Moriyama *et al*, 2018). In addition to conserved interaction with PP1, Rif1 is known to interact with a number of proteins. *S.pombe* Rif1 interacts with telomere factors Taz1 and Rap1 (Kanoh & Ishikawa, 2001; Miller *et al*, 2005). This interaction is important for its function at the telomere. It also interacts with Epe1 (Wang *et al*, 2013), Jmjc domain chromatin associated protein, suggesting its potential role in chromatin regulation. Human Rif1 interacts with DSB repair factors, 53BP1, Mdc1, Bloom RecQ helicase (Batenburg *et al*, 2017; Gupta *et al*, 2018; Feng *et al*, 2013), and anti-silencing function 1B histone chaperone, ASF1B (Huttlin *et al*, 2017). This underscores its roles in regulation of DSB repair and epigenomic state. Both fission yeast and human Rif1 are biochemically enriched in nuclear insoluble fractions, and a portion of mammalian Rif1 is localized at nuclear periphery. It was speculated that Rif1 tethers chromatin fiber along the nuclear membrane, generating a chromatin compartment in the vicinity of nuclear periphery (Kobayashi *et al.*, 2019; Yamazaki *et al.*, 2012). However, effects of the increased level of Rif1 on chromatin localization in nuclei and its subsequent outcome have not been explored.

In this communication, we showed that increased numbers of Rif1 molecules in fission yeast cells stimulated its chromatin arm binding and relocation of chromatin to nuclear periphery/ detergent-insoluble compartments, leading to cell death induced by aberrant mitosis. Rif1 overexpression inhibited also S phase, and this inhibition depends on the interaction with PP1, while PP1 was not required for chromatin relocation and growth inhibition by Rif1.

Events induced by overexpression of Rif1 in fission yeast cells.

We observed severe growth inhibition of fission yeast cells by overexpression of Rif1 protein. The growth inhibition was observed only on the plate lacking thiamine where the nmt1 promoter driving the transcription of plasmid-borne Rif1 is activated. We detected ~1,000 molecules of Rif1 protein in a growing fission yeast cell. It increased

by 10 fold in cells harboring the plasmid expressing Rif1, and upon depletion of thiamine, it increased further by 3.7 fold. Thus, the presence of Rif1 over the threshold (between ~10,000 and ~3,7000 molecules per cell) may confer the growth inhibition. Rif1 overexpression delayed S phase initiation and progression in synchronized cell populations. Interestingly, S phase inhibition was not observed by overexpression of the PP1bs mutant of Rif1, indicating that inhibition of DNA synthesis depends on the recruitment of PP1 (**Fig 3A**). Replication checkpoint, as measured by Cds1 kinase activity, was activated by overexpression of the PP1bs mutant of Rif1 protein, but not by the wild-type Rif1 protein (**Fig 3C**). This could be due to the ongoing S phase in PP1bs mutant-overexpressing cells while S phase is inhibited by the wild-type Rif1. Ongoing replication forks would be interfered by the bound Rif1 proteins, activating replication checkpoint. On the other hand, in the wild-type Rif1 overexpression, initiation of DNA synthesis is blocked by Rif1, thus generating less fork blocks, i.e. less replication checkpoint activation.

Cells with short spindles accumulate in Rif1-overproduced cells, and this incident depends on SAC (**Fig 5B**). Growth inhibition is observed in SAC mutant cells, indicating that short spindle formation is not critical for growth inhibition. Rather, severer growth inhibition was observed in the SAC mutants. Short spindles were reported to accumulate in SAC activated cells, and it was reported that replication intermediates or recombination-intermediates can activate SAC (Nakano *et al*, 2014), resulting in cells with short spindles. SAC was less efficiently activated by overexpression of a PP1bs mutant, consistent with reduced short spindles in this mutant. As stated above, Rif1 inhibited growth more strongly in SAC mutants than in the wild-type cells. The PP1bs mutant inhibited growth slightly more strongly than the wild-type Rif1. These results indicate that SAC-induced mitotic arrest with short spindles may serve as a protective barrier against aberrant mitosis that would lead to cell death (**Fig 9**).

Aberrant chromatin structures induced by Rif1 suggests the ability of Rif1 to tether chromatin at nuclear periphery

Histone H3 (H3.2) labeled chromatin is detected uniformly in nuclei in the wild-type cells. Upon overexpression of Rif1 protein, nuclei with chromatin enriched at the nuclear periphery were observed in more than 6% or 10% of the cells with the wild-type

or PP1bs mutant Rif1, respectively. Furthermore, chromatin binding-deficient mutant, L848S, failed to induce chromatin relocation to nuclear periphery (**Fig 7**).

By using a Rif1 derivative containing mKO2 between the HEAT repeat and C-terminal segment, cellular Rif1 dynamics was examined. In addition to the strong dots corresponding to telomeres (**Fig S5D and E**), fine dots representing arm binding were observed ((Klein *et al.*, 2021)**Supplementary movie**). Upon overexpression of Rif1, the endogenous Rif1-derived mKO2 signals relocated from telomeres to the entire areas of nuclei (**Fig S5E**), indicating that overexpressed Rif1, forming multimers with Rif1-mKO2, spreads over the chromosome arms. The prewash of nuclei with detergent and DNase I enhanced the Rif1 signals in nuclei, notably at nuclear periphery (**Fig S6B**). Both the numbers of foci and overall intensities of nuclear signals increased upon Rif1 overproduction (**Fig 8B and C**), presumably due to relocation of endogenous Rif1 from telomere to chromosome arms and to detergent- and DNase I-resistant insoluble compartments through mixed oligomer formation with the overexpressed Rif1.

Our results are consistent with the idea that Rif1 promotes association of chromatin with detergent-insoluble membrane fractions, which are known to be enriched with S-acylated proteins (Hooper, 1999). Like budding yeast Rif1, fission yeast Rif1 may also be S-acylated (Fontana *et al.*, 2019).

Mechanisms of formation of aberrant microtubule spindles

Rif1 overexpression ultimately induces cell death through aberrant mitosis. In addition to cells with short spindles, those with aberrant defective microtubules appear. The fractions of these cells increase in PP1 mutant cells as well as in PP1bs mutant-overproducing cells. PP1-Rif1 interaction is regulated by phosphorylation of Rif1 and Aurora B kinase was reported to play a major role in phosphorylating the PP1bs, promoting the dissociation of PP1 from Rif1 during M phase (Bhowmick *et al*, 2019; Nasa *et al*, 2018). Overexpressed Rif1 would recruit PP1, counteracting the phosphorylation events by Aurora B and other kinases essential for mitosis. This may lead to misconduct in mitotic events. However, since PP1bs mutants can also cause aberrant microtubules and cell death, PP1 may not be the primary cause for aberrant microtubule cell death. The aberrant chromatin structure caused by overexpressed Rif1 may affect the mitotic chromatin structure, leading to mitotic defect. Alternatively, the

aberrant association of Rif1 with mitotic kinases and potentially with microtubules could directly be linked to deficient microtubules in Rif1-overproducing cells.

In summary, overexpression of Rif1 would lead to relocation of the chromatin segment located in the interior of nuclei (early-replicating loci) to nuclear periphery. Replication of DNA in the vicinity of tethered chromatin segment would be inhibited upon recruitment of PP1. It was previously reported that artificial tethering of an early-firing origin at nuclear periphery did not render it late-firing in budding yeast (Ebrahimi *et al*, 2010). This is consistent with our result that Rif1-mediated chromatin recruitment at nuclear membrane alone does not inhibit S phase, and that the recruitment of PP1 by Rif1 is required for the inhibition. On the other hand, recruitment of chromatin to the nuclear periphery by Rif1 is sufficient to cause aberrant M phase and eventually cell death. The results described in this report support the idea that Rif1-mediated chromatin association with nuclear periphery needs to be precisely regulated for coordinated progression of S and M phase. However, we cannot rule out the possibility that the phenotypes we observe upon Rif1 overexpression could be secondary consequences of its effect on transcription or on other chromosomal events including repair and recombination. More detailed studies will be needed to precisely determine the effects of deregulated chromatin association with nuclear membrane on cell cycle progression and cell survival.

Material and Methods

Medium for *Schizosaccharomyces pombe*

YES media contains 0.5 % yeast extract (Gibco), 3 % glucose (FUJIFILM Wako) and 0.1 mg/mL each of adenine (Sigma-Aldrich), uracil (Sigma -Aldrich), leucine (FUJIFILM Wako), lysine (FUJIFILM Wako) and histidine (FUJIFILM Wako). YES plates were made by adding 2 % agar (Gibco) to YES media. Synthetic dextrose minimal medium (SD) contains 6.3 g/L Yeast Nitrogen Base w/o Amino Acids (BD), 2% glucose and 0.1 mg/mL each of required amino acids. Edinburgh Minimal Medium (EMM) contains 12.3 g/L EMM BROTH WITHOUT NITROGEN (FORMEIUM), 2% glucose and 0.1 mg/mL each of required amino acids. Pombe Minimal Glutamate (PMG) contains 27.3 g/L EMM BROTH WITHOUT NITROGEN, 5 g/L L-glutamic acid (Sigma-Aldrich) and 0.1 mg/mL each of required amino acids. Fifteen μM thiamine (Sigma-Aldrich) was added to EMM or PMG medium to repress the nmt1 promoter activity. Yeast strains and plasmids used in this study are listed in **Table 1** and **Table 2**.

Synchronization and cell cycle analysis by Flow Cytometry

Rif1-expression in the yeasts containing *nda3-KM311* mutation (KYP1268, MS733 and KYP1283) was inducted for 12 hr in PMG medium without thiamine. The yeasts were arrested at 20 ºC for 6 hr and then the cells were synchronization at M-phase and Rif1-expression inducted for 18 hr. They were released into sub-sequential cell cycle at 30 ºC. Cells in 5 mL culture were collected and suspended in 200 μL water. Cells were fixed with 600 μL ethanol, washed with 50 mM sodium citrate (pH7.5) (FUJIFILM Wako), and were treated with 0.1 mg/mL RNase A (Sigma-Aldrich) in 300 μL of 50 mM sodium citrate at 37 ºC for 2 hr. Cells were stained with 4 ng/mL propidium iodide (Sigma-Aldrich) at room temperature for 1 hr. After sonication, cells were analyzed by BD LSRFortessaTM X-20.

Co-immunoprecipitation

The procedure was performed as described previously (Shimmoto *et al*, 2009). For immunoprecipitation, approximately 1.0 $\times 10^8$ cells from 50 mL culture were harvested and washed once with PBS. The cells were then resuspended in 0.5 mL of IP buffer (20 mM HEPES-KOH [pH 7.6] (Nacalai tesque), 50 mM potassium acetate (Sigma-Aldrich),

5 mM magnesium acetate (FUJIFILM Wako), 0.1 M sorbitol (FUJIFILM Wako), 0.1% TritonX-100 (Sigma-Aldrich), 2 mM DTT (FUJIFILM Wako), 20 mM Na_3VO_4 (Sigma-Aldrich), 50 mM β-glycerophosphate (Sigma-Aldrich) and Protease Inhibitor Cocktail (Sigma-Aldrich)) and were disrupted with glass beads using a Multi-Beads Shocker (Yasui Kikai; Osaka, Japan). The lysates were cleared by centrifugation (15,000 rpm for 10 min at 4 ºC). The supernatants of lysates were mixed with anti-c-Myc antibody (Nacalai tesque) attached to Protein G Dynabeads™ (Thermo Fisher, 10004D). After incubation for 1 hr, beads were washed with IP buffer and proteins were extracted by boiling with 1× sample buffer (2% SDS (Nacalai tesque), 4 M Urea (Nacalai tesque), 60 mM Tris-HCl [pH6.8] (Nacalai tesque), 10% Glycerol (nacalai tesque), and 70 mM 2-Mercaptethanol (Sigma-Aldrich)].

Immunoblot

Protein samples and prestained molecular weight markers (Bio-Rad) were loaded onto 5~20% gradient precast PAGE gel (ATTO corp.), and transferred to PVDF membranes (Millipore). The membranes were blocked with 5% skim milk in TBST and target proteins were detected with ANTI-FLAG® M2 antibody (Sigma-Aldrich) and anti-α-Tubulin (SantaCruz).

Chromatin immunoprecipitation (ChIP)

1.0×10^9 cells were cross-linked with 1% formaldehyde for 15 min at 30 ºC, and prepared for ChIP as previously described (Kanoh *et al.*, 2015; Katou *et al*, 2003). Briefly, cross-linked cell lysates prepared by multi-beads shocker (Yasui Kikai Co.) and sonication (Branson) were incubated with Protein G Dynabeads™ (Thermo Fisher, 10004D) attached to ANTI-FLAG® M2 antibody (Sigma-Aldrich) for 4 hr at 4 °C. The beads were washed several times and the precipitated materials were eluted by incubation in elution buffer (50 mM Tris-HCl [pH7.6], 10 mM EDTA and 1 % SDS) for 20 min at 68 °C. The eluates were incubated at 68 °C overnight to reverse crosslinks and then treated with RNaseA (Sigma-Aldrich) and proteinase K (FUJIFILM Wako). DNA was precipitated with ethanol in the presence of glycogen (Nacalai tesque) and further purified by using QIAquick PCR purification kit (Qiagen).

Living cell analysis

Cells were observed on BZ-X700 (KEYENCE) equipped with Nikon PlanApoλ 100× (NA=1.45) using IMMERSION OIL TYPE NF2 (Nikon). Mitotic spindles were visualized by expressing Pmt1-GFP-α-Tubulin. DNA damages were detected by observing fluorescent Rad52 foci (EGFP or YFP). Securin and spindle pole bodies were visualized by expressing Cut2-GFP and Sad1-GFP, respectively. The time-lapse images were observed on PMG medium/ 2% agarose (Nacalai tesque). Whole chromosome locations were visualized by expressing hht2 (Histone H3 h3.2)-GFP.

Next generation sequencing (NGS) and ChIP-Seq

NGS libraries were prepared as described previously (Kanoh *et al.*, 2015). The input and the immunoprecipitated DNAs were fragmented to an average size of approximately150 bp by ultra-sonication (Covaris). The fragmented DNAs were end-repaired, ligated to sequencing adapters and amplified using NEBNext® Ultra™ II DNA Library Prep Kit for Illumina® and NEBNext Multiplex Oligos for Illumina® (New England Biolabs). The amplified DNA (around 275 bp in size) was sequenced on Illumina MiSeq to generate single reads of 100 bp. The generated ChIP or Input sequences were aligned to the *S. pombe* genomic reference sequence provided from PomBase by Bowtie 1.0.0 using default setting. Peaks were called with Model-based analysis of ChIP-Seq (MACS2.0.10) using following parameters; macs2 callpeak -t ChIP.sam -c Input.sam -f SAM -g $1.4e10^7$ -n result_file –B -q 0.01. The pileup graphs were loaded on Affymetrix Integrated Genome Browser (IGB 8.0). To identify consensus conserved sequences for Rif1-binding, 300 bp DNA segments around the summits of the 128 or 169 Rif1 binding sites identified by MACS2 were extracted and analyzed by MEME suite (Bailey *et al*, 2015).

In-gel kinase assay

In-gel kinase assays for replication checkpoint activation were conducted as described previously (Geahlen *et al*, 1986; Takeda *et al*, 2001; Waddell *et al*, 1995).
SDS-polyacrylamide gel (10%) was cast in the presence of 0.5 mg/ml myelin basic protein (Sigma) within the gel. Extracts (100 μg of protein) prepared by the boiling method were run on the gel. After electrophoresis, the gel was washed successively in 50 mM Tris-HCl (pH 8.0), 50 mM Tris-HCl (pH 8.0)+5 mM 2-mercaptoethanol, and

denatured in 6 M guanidium hydrochloride (Nacalai tesque) in 50 mM Tris-HCl (pH 8.0)+5 mM 2-mercaptoethanol, and renatured in 50 mM Tris, pH 8.0+5 mM 2-mercaptoethanol+0.04% Tween 20 over 12-18 h at 4°C. The gel was then equilibrated in the kinase buffer containing 40 mM HEPES-KOH (pH 7.6), 40 mM potassium glutamate, 5 mM magnesium acetate, 2 mM dithiothreitol, and 0.1 mM EGTA for 1 h at room temperature, and was incubated in the same kinase buffer containing 5 μ□M ATP and 50 μCi of [γ□-^{32}P]ATP for 60 min at room temperature, followed by extensive washing in 5% trichloro- acetic acid (Nacalai tesque)+1% sodium pyrophosphate until no radioactivity is detected in the washing buffer. The gel was dried and autoradiographed.

Cell fractionation and immunofluorescence analyses

5.0×10^7 exponentially growing yeast cells were collected, and cell components were fractionated as previously reported (Kanoh *et al.*, 2015). Briefly, the cell walls were digested with 100 U/ml zymolyase (Nacalai Tesque) in 1.2 M sorbitol/ potassium phosphate (pH7.0) containing 1 mM PMSF at 30°C for 30 min. The spheroplast cells, washed with 1 M sorbitol, were permeabilized in a solution containing 0.1% Triton X-100 (Sigma-Aldrich), 1.2 M sorbitol/ potassium phosphate (pH 7.0) and 1 mM PMSF on ice. The cells were suspended in CSK buffer (50 mM HEPES-KOH [pH 7.5], 0.5% Triton X-100, 50 mM potassium acetate, 1 mM MgCl2, 1 mM EDTA, 1 mM EGTA, 1 mM DTT, 1 mM PMSF, 0.5 mM sodium orthovanadate, 50 mM NaF, 1× protease-inhibitor cocktail (Sigma-Aldrich), 1× protease-inhibitor cocktail (Roche), and 0.1 mM MG-132) for 30 min on ice. Genomic DNA was digested with 0.25 U/ml DNase I in CSK buffer containing 10 mM $MgCl_2$ and 10 mM $CaCl_2$ and incubated at 20°C for 30 min. The cells were fixed with 4% paraformaldehyde/ PBS after wash with CSK buffer. Nup98, a marker of the nuclear membrane, was detected with rat anti-Nup98 monoclonal antibody (1:500; Bioacademia) for 12 hr at 4°C after blocking in PBS containing 3% BSA and 0.1% Tween 20. The cells were washed with PBS containing 0.1% Tween 20 three times, and were incubated with Alexa Fluor 488–conjugated rabbit anti–rat IgG (1:1000; Invitrogen) in PBS containing 0.1% Tween 20 for 12 hr at 4°C. Antibodies were diluted in 1% BSA in PBS and 0.1% Tween 20.

Finally, the cells were stained with 1 μg/mL Hoechst® 33342 for 1 hr at r.t. and washed with PBS containing 0.5% Tween 20 three times before visualization under microscope.

Time laps analyses of cellular dynamics of Rif1

Cells expressing Rif1-mKO2 (red) and Taz1-EGFP (green) at the endogenous loci were analyzed under spinning disk microscope. Images were taken as previously reported (Ito *et al*, 2019) with slight modification. Briefly, microscope images were acquired using an iXon3 897 EMCCD camera (Andor) connected to Yokokawa CSU-W1 spinning-disc scan head (Yokokawa Electric Corporation) and an OlympusIX83 microscope (Olympus) with a UPlanSApo 100× NA 1.4 objective lens (Olympus) with laser illumination at 488 nm for GFP and 561 nm for mKO2. Images were captured and analyzed using MetaMorph Software (Molecular Devices). Optical section data (41 focal planes with 0.2 μm spacing every 2 min) were collected for 2 hr. Time-lapse images were deconvoluted using Huygens image analysis software (Scientific Volume Imaging).

Estimation of the number of the Rif1 molecule in fission yeast cells.

His_6-Rif1-$Flag_3$ (93-1400aa) protein was expressed on ver.3-4 vector at the BamHI site, and was purified by the consecutive anti-Flag column and nickel column (Uno *et al*, 2012). The N-terminal 93 amino acids were removed to increase the stability of the protein. The whole cell extracts prepared by the boiling method (Takeda *et al.*, 2001) from the cells of known numbers were serially diluted, and run on PAGE together with the standard protein of the known concentrations, the purified His_6-Rif1-$Flag_3$ protein.

Data Availability

The reagents, oligonucleotides, plasmids, strains and Rif1 binding sequence lists used in this study are listed in **Tables 1~5**.

Acknowledgements

We thank Kenji Moriyama for providing the purified N-terminally truncated fission yeast Rif1 protein (93-1400aa). We also thank Rino Fukatsu and Naoko Kakusho for excellent technical assistance. We thank Dr. Justin O'Sullivan for providing us with the

data on prediction of nuclear localization of Rif1 and DNA replication in fission yeast cells. We thank Prof. Takashi Toda (Hiroshima University) for helpful suggestions. This paper is dedicated to Dr. Seiji Matsumoto, a dearest friend and collaborator, who passed away on November 22, 2020, after a long fight against pancreatic cancer.

Author Contributions

Y.K. conducted plasmid and mutant strain constructions, observed mutants by microscope, analyzed cell cycle by FACS, and conducted ChIP-seq and informatics analyses. S.M. and M.H. also constructed plasmids and mutant strains, characterized them, and conducted immunoprecipitation and data analysis. M.H. and S.K. found that Rif1 overexpression induced cell death. M.U. provided mutant strains, conducted live cell analyses and interpreted the data. Y.K., S.M. and H.M. conceived and designed the experiments and Y.K. and H.M. wrote the paper.

Conflict of interest

The authors declare that they have no conflict of interest.

References

Amiad-Pavlov D, Lorber D, Bajpai G, Reuveny A, Roncato F, Alon R, Safran S, Volk T (2021) Live imaging of chromatin distribution reveals novel principles of nuclear architecture and chromatin compartmentalization. *Sci Adv* 7

Arib G, Akhtar A (2011) Multiple facets of nuclear periphery in gene expression control. *Curr Opin Cell Biol* 23: 346-353

Bailey TL, Johnson J, Grant CE, Noble WS (2015) The MEME Suite. *Nucleic Acids Res* 43: W39-49

Batenburg, N. L., Walker, J. R., Noordermeer, S. M., Moatti, N., Durocher, D., & Zhu, X. D. (2017). ATM and CDK2 control chromatin remodeler CSB to inhibit RIF1 in DSB repair pathway choice. *Nat Commun, 8*(1), 1921. doi:10.1038/s41467-017-02114-x

Bernard P, Hardwick K, Javerzat JP (1998) Fission yeast bub1 is a mitotic centromere protein essential for the spindle checkpoint and the preservation of correct ploidy through mitosis. *The Journal of cell biology* 143: 1775-1787

Bernard P, Maure JF, Javerzat JP (2001) Fission yeast Bub1 is essential in setting up the meiotic pattern of chromosome segregation. *Nat Cell Biol* 3: 522-526

Bhowmick R, Thakur RS, Venegas AB, Liu Y, Nilsson J, Barisic M, Hickson ID (2019) The RIF1-PP1 Axis Controls Abscission Timing in Human Cells. *Curr Biol* 29: 1232-1242 e1235

Campolo F, Gori M, Favaro R, Nicolis S, Pellegrini M, Botti F, Rossi P, Jannini EA, Dolci S (2013) Essential role of Sox2 for the establishment and maintenance of the germ cell line. *Stem Cells* 31: 1408-1421

Cornacchia D, Dileep V, Quivy JP, Foti R, Tili F, Santarella-Mellwig R, Antony C, Almouzni G, Gilbert DM, Buonomo SB (2012) Mouse Rif1 is a key regulator of the replication-timing programme in mammalian cells. *The EMBO journal* 31: 3678-3690

Dave A, Cooley C, Garg M, Bianchi A (2014) Protein phosphatase 1 recruitment by Rif1 regulates DNA replication origin firing by counteracting DDK activity. *Cell Rep* 7: 53-61

Di Virgilio M, Callen E, Yamane A, Zhang W, Jankovic M, Gitlin AD, Feldhahn N, Resch W, Oliveira TY, Chait BT *et al* (2013) Rif1 prevents resection of DNA breaks and promotes immunoglobulin class switching. *Science* 339: 711-715

Du LL, Nakamura TM, Moser BA, Russell P (2003) Retention but not recruitment of Crb2 at double-strand breaks requires Rad1 and Rad3 complexes. *Molecular and cellular biology* 23: 6150-6158

Ebrahimi H, Robertson ED, Taddei A, Gasser SM, Donaldson AD, Hiraga S (2010) Early initiation of a replication origin tethered at the nuclear periphery. *J Cell Sci* 123: 1015-1019

Feng, L., Fong, K. W., Wang, J., Wang, W., & Chen, J. (2013). RIF1 counteracts BRCA1-mediated end resection during DNA repair. *J Biol Chem, 288*(16), 11135-11143. doi:10.1074/jbc.M113.457440

Fontana GA, Hess D, Reinert JK, Mattarocci S, Falquet B, Klein D, Shore D, Thoma NH, Rass U (2019) Rif1 S-acylation mediates DNA double-strand break repair at the inner nuclear membrane. *Nat Commun* 10: 2535

Foti R, Gnan S, Cornacchia D, Dileep V, Bulut-Karslioglu A, Diehl S, Buness A, Klein FA, Huber W, Johnstone E *et al* (2016) Nuclear Architecture Organized by Rif1 Underpins the Replication-Timing Program. *Molecular cell* 61: 260-273

Furuya K, Carr AM (2003) DNA checkpoints in fission yeast. *J Cell Sci* 116: 3847-3848

Garcia MA, Vardy L, Koonrugsa N, Toda T (2001) Fission yeast ch-TOG/XMAP215 homologue Alp14 connects mitotic spindles with the kinetochore and is a component of the Mad2-dependent spindle checkpoint. *The EMBO journal* 20: 3389-3401

Geahlen RL, Anostario M, Jr., Low PS, Harrison ML (1986) Detection of protein kinase activity in sodium dodecyl sulfate-polyacrylamide gels. *Anal Biochem* 153: 151-158

Gupta, R., Somyajit, K., Narita, T., Maskey, E., Stanlie, A., Kremer, M., . . . Choudhary, C. (2018). DNA Repair Network Analysis Reveals Shieldin as a Key Regulator of NHEJ and PARP Inhibitor Sensitivity. *Cell, 173*(4), 972-988 e923. doi:10.1016/j.cell.2018.03.050

Hayano M, Kanoh Y, Matsumoto S, Renard-Guillet C, Shirahige K, Masai H (2012) Rif1 is a global regulator of timing of replication origin firing in fission yeast. *Genes & development* 26: 137-150

Hiraga S, Alvino GM, Chang F, Lian HY, Sridhar A, Kubota T, Brewer BJ, Weinreich M, Raghuraman MK, Donaldson AD (2014) Rif1 controls DNA replication by directing Protein Phosphatase 1 to reverse Cdc7-mediated phosphorylation of the MCM complex. *Genes & development* 28: 372-383

Hooper NM (1999) Detergent-insoluble glycosphingolipid/cholesterol-rich membrane

domains, lipid rafts and caveolae (review). *Mol Membr Biol* 16: 145-156
Huttlin, E. L., Bruckner, R. J., Paulo, J. A., Cannon, J. R., Ting, L., Baltier, K., . . . Harper, J. W. (2017). Architecture of the human interactome defines protein communities and disease networks. *Nature, 545*(7655), 505-509. doi:10.1038/nature22366
Iino Y, Yamamoto M (1997) The Schizosaccharomyces pombe cdc6 gene encodes the catalytic subunit of DNA polymerase delta. *Mol Gen Genet* 254: 93-97
Ikui AE, Furuya K, Yanagida M, Matsumoto T (2002) Control of localization of a spindle checkpoint protein, Mad2, in fission yeast. *J Cell Sci* 115: 1603-1610
Ito H, Sugawara T, Shinkai S, Mizukawa S, Kondo A, Senda H, Sawai K, Ito K, Suzuki S, Takaine M *et al* (2019) Spindle pole body movement is affected by glucose and ammonium chloride in fission yeast. *Biochem Biophys Res Commun* 511: 820-825
Jumper J, Evans R, Pritzel A, Green T, Figurnov M, Ronneberger O, Tunyasuvunakool K, Bates R, Zidek A, Potapenko A *et al* (2021) Highly accurate protein structure prediction with AlphaFold. *Nature* 596: 583-589
Kanoh J, Ishikawa F (2001) spRap1 and spRif1, recruited to telomeres by Taz1, are essential for telomere function in fission yeast. *Curr Biol* 11: 1624-1630
Kanoh Y, Matsumoto S, Fukatsu R, Kakusho N, Kono N, Renard-Guillet C, Masuda K, Iida K, Nagasawa K, Shirahige K *et al* (2015) Rif1 binds to G quadruplexes and suppresses replication over long distances. *Nature structural & molecular biology* 22: 889-897
Katou Y, Kanoh Y, Bando M, Noguchi H, Tanaka H, Ashikari T, Sugimoto K, Shirahige K (2003) S-phase checkpoint proteins Tof1 and Mrc1 form a stable replication-pausing complex. *Nature* 424: 1078-1083
Kinoshita N, Ohkura H, Yanagida M (1990) Distinct, essential roles of type 1 and 2A protein phosphatases in the control of the fission yeast cell division cycle. *Cell* 63: 405-415
Klein KN, Zhao PA, Lyu X, Sasaki T, Bartlett DA, Singh AM, Tasan I, Zhang M, Watts LP, Hiraga SI *et al* (2021) Replication timing maintains the global epigenetic state in human cells. *Science* 372: 371-378
Kobayashi S, Fukatsu R, Kanoh Y, Kakusho N, Matsumoto S, Chaen S, Masai H (2019) Both a Unique Motif at the C Terminus and an N-Terminal HEAT Repeat Contribute to G-Quadruplex Binding and Origin Regulation by the Rif1 Protein. *Molecular and*

cellular biology 39
Kumar S, Huberman JA (2004) On the slowing of S phase in response to DNA damage in fission yeast. *J Biol Chem* 279: 43574-43580
Laghmach R, Di Pierro M, Potoyan DA (2021) The interplay of chromatin phase separation and lamina interactions in nuclear organization. *Biophys J* 120: 5005-5017
Lemaitre C, Bickmore WA (2015) Chromatin at the nuclear periphery and the regulation of genome functions. *Histochem Cell Biol* 144: 111-122
Mahamid J, Pfeffer S, Schaffer M, Villa E, Danev R, Cuellar LK, Forster F, Hyman AA, Plitzko JM, Baumeister W (2016) Visualizing the molecular sociology at the HeLa cell nuclear periphery. *Science* 351: 969-972
Masai H, Fukatsu R, Kakusho N, Kanoh Y, Moriyama K, Ma Y, Iida K, Nagasawa K (2019) Rif1 promotes association of G-quadruplex (G4) by its specific G4 binding and oligomerization activities. *Sci Rep* 9: 8618
Matsumoto S, Ogino K, Noguchi E, Russell P, Masai H (2005) Hsk1-Dfp1/Him1, the Cdc7-Dbf4 kinase in Schizosaccharomyces pombe, associates with Swi1, a component of the replication fork protection complex. *J Biol Chem* 280: 42536-42542
Mattarocci S, Shyian M, Lemmens L, Damay P, Altintas DM, Shi T, Bartholomew CR, Thoma NH, Hardy CF, Shore D (2014) Rif1 controls DNA replication timing in yeast through the PP1 phosphatase Glc7. *Cell Rep* 7: 62-69
Miller, K. M., Ferreira, M. G., & Cooper, J. P. (2005). Taz1, Rap1 and Rif1 act both interdependently and independently to maintain telomeres. *Embo j, 24*(17), 3128-3135. doi:10.1038/sj.emboj.7600779
Moriyama K, Yoshizawa-Sugata N, Masai H (2018) Oligomer formation and G-quadruplex binding by purified murine Rif1 protein, a key organizer of higher-order chromatin architecture. *J Biol Chem* 293: 3607-3624
Nakano A, Masuda K, Hiromoto T, Takahashi K, Matsumoto Y, Habib AG, Darwish AG, Yukawa M, Tsuchiya E, Ueno M (2014) Rad51-dependent aberrant chromosome structures at telomeres and ribosomal DNA activate the spindle assembly checkpoint. *Molecular and cellular biology* 34: 1389-1397
Nasa I, Rusin SF, Kettenbach AN, Moorhead GB (2018) Aurora B opposes PP1 function in mitosis by phosphorylating the conserved PP1-binding RVxF motif in PP1 regulatory proteins. *Sci Signal* 11
Park S, Patterson EE, Cobb J, Audhya A, Gartenberg MR, Fox CA (2011)

Palmitoylation controls the dynamics of budding-yeast heterochromatin via the telomere-binding protein Rif1. *Proc Natl Acad Sci U S A* 108: 14572-14577

Ptak C, Wozniak RW (2016) Nucleoporins and chromatin metabolism. *Curr Opin Cell Biol* 40: 153-160

Rowley R, Hudson J, Young PG (1992) The wee1 protein kinase is required for radiation-induced mitotic delay. *Nature* 356: 353-355

See K, Kiseleva AA, Smith CL, Liu F, Li J, Poleshko A, Epstein JA (2020) Histone methyltransferase activity programs nuclear peripheral genome positioning. *Dev Biol* 466: 90-98

Shimmoto M, Matsumoto S, Odagiri Y, Noguchi E, Russell P, Masai H (2009) Interactions between Swi1-Swi3, Mrc1 and S phase kinase, Hsk1 may regulate cellular responses to stalled replication forks in fission yeast. *Genes Cells* 14: 669-682

Shyian M, Mattarocci S, Albert B, Hafner L, Lezaja A, Costanzo M, Boone C, Shore D (2016) Budding Yeast Rif1 Controls Genome Integrity by Inhibiting rDNA Replication. *PLoS Genet* 12: e1006414

Smith CL, Poleshko A, Epstein JA (2021) The nuclear periphery is a scaffold for tissue-specific enhancers. *Nucleic Acids Res* 49: 6181-6195

Takeda T, Ogino K, Tatebayashi K, Ikeda H, Arai K, Masai H (2001) Regulation of initiation of S phase, replication checkpoint signaling, and maintenance of mitotic chromosome structures during S phase by Hsk1 kinase in the fission yeast. *Mol Biol Cell* 12: 1257-1274

Uno S, You Z, Masai H (2012) Purification of replication factors using insect and mammalian cell expression systems. *Methods* 57: 214-221

Waddell TK, Fialkow L, Chan CK, Kishimoto TK, Downey GP (1995) Signaling functions of L-selectin. Enhancement of tyrosine phosphorylation and activation of MAP kinase. *J Biol Chem* 270: 15403-15411

Wang, J., Tadeo, X., Hou, H., Tu, P. G., Thompson, J., Yates, J. R., 3rd, & Jia, S. (2013). Epe1 recruits BET family bromodomain protein Bdf2 to establish heterochromatin boundaries. *Genes Dev, 27*(17), 1886-1902. doi:10.1101/gad.221010.113

Yamazaki S, Ishii A, Kanoh Y, Oda M, Nishito Y, Masai H (2012) Rif1 regulates the replication timing domains on the human genome. *The EMBO journal* 31: 3667-3677

Yoshizawa-Sugata N, Yamazaki S, Mita-Yoshida K, Ono T, Nishito Y, Masai H (2021)

Loss of full-length DNA replication regulator Rif1 in two-cell embryos is associated with zygotic transcriptional activation. *J Biol Chem* 297: 101367

Zaaijer S, Shiakh N, Nageshan RK., Cooper JP (2016) "Rif1 regulates the fate of DNA entanglements during mitosis." *Cell Report* 16: 148-160.

Zimmermann M, Lottersberger F, Buonomo SB, Sfeir A, de Lange T (2013) 53BP1 regulates DSB repair using Rif1 to control 5' end resection. *Science* 339: 700-704

Legends to Figures

Figure 1. Overexpression of Rif1 inhibits growth of fission yeast cells.

(A) Time course of overexpression of Rif1-Flag$_3$ protein expressed on pREP41 plasmid under the nmt41promoter after transfer to medium lacking thiamine (lanes 3-9)(KYP008 + pREP41-Rif1-Flag$_3$). Lanes 1 and 2 (HM511 + pREP41), Rif1-Flag$_3$ is expressed at the endogenous *rif1* locus under its own promoter in the presence or absence of thiamine in the medium. Proteins were detected by the anti-Flag antibody.

(B) Schematic drawing of deletion derivatives of Rif1 protein analyzed in this study (KYP008 + pREP41-Rif1 truncation series in **Table 2**). + indicates growth inhibition, whereas – indicates the absence of growth inhibition. The PP1 binding motifs (RVxF and SILK) are indicated in red and blue, respectively. Note that the motifs in Rif1 are slightly diverged from the above consensus sequences. The polypeptide segments capable of G4 binding and oligomerization are also indicated.

(C, D) Effects of overexpression of the full length and truncated mutants of Rif1 were examined. Proteins were expressed on pREP41 in medium containing (+Thi) or lacking (–Thi) thiamine. Serially diluted (5× fold) cells were spotted and growth of the spotted cells was examined after incubation at the indicated temperature for the indicated time. Growth inhibition was observed with full-length (1-1400) (KYP1805), 1-1260 (KYP1853), 61-1400 (KYP1806) or 81-1400 (KYP1807) derivatives of Rif1.

Figure 2. PP1-Rif1 interaction is not required for the growth inhibition caused by Rif1 overexpression.

(A) Spot tests of Rif1 overexpression in the PP1 mutants *dis2*Δ (KYP1762), *dis2-11* (KYP1760) or *sds21*Δ (KYP1764) cells were conducted as described in **Fig 1C and D**. Rif1 overexpression inhibited growth of the mutant cells similar to the wild type cells.

(B) Mutations introduced at the PP1 binding sites (RVxF and SILK motif) of Rif1.

(C) Using the extracts made from the cells expressing both Flag-tagged Rif1 and Myc-tagged PP1 (Dis2 or Sds21) (KYP1769, KYP1770, KYP1772 and KYP1773), PP1 were immunoprecipitated by anti-Myc antibody, and co-immunoprecipitated Rif1 were detected. The PP1bs mutant of Rif1 does not interact with either PP1.

(D) Time course of overexpression of *rif1*PP1bsmut-Flag$_3$ protein expressed on pREP41 plasmid under the nmt41 promoter after transfer to medium lacking thiamine (lanes 3-9)

(KYP1839). Lanes 1 and 2 (KYP1827), *rif1*PP1bsmut -Flag$_3$ is expressed at the endogenous *rif1* locus under its own promoter in the presence or absence of thiamine in the medium.

(E) Spot tests of the wild-type (KYP025, KYP015 and KYP1774) and *rif1*Δ (KYP1804, KYP1805 and KYP1839) cells overexpressing the wild-type or a PP1bs mutant. Overexpression of the PP1bs mutant Rif1 inhibited growth of fission yeast cells in a manner similar to or slightly better than the wild-type Rif1 did.

Figure 3. Effect of overexpression of Rif1 protein on cell cycle progression and replication checkpoint activation.

(A) The *nda3-KM311* cold-sensitive mutant cells with wild-type *rif1*$^+$ (KYP1268) or those expressing the wild-type Rif1 (Pnmt41-Rif1) (MS733) or PP1bs mutant Rif1 (Pnmt41-*rif1*PP1bsmut) (KYP1283) at the endogenous *rif1* locus under nmt41 promoter were arrested at M-phase by incubation at 20°C for 6 hr with concomitant depletion of thiamine. The cells were released into cell cycle at 30°C. The cell cycle progression was monitored by flow cytometry. The cells with Pnmt41-*rif1*PP1bsmut entered S-phase at 30 min (at 18.5 hr in FACS chart) after release from M-phase arrest, similar to the *rif1*$^+$ cells, whereas those with Pnmt41-Rif1 entered S-phase later (>60 min after release).

(B) The level of Rif1 in the samples from (**A**) was examined by western blotting.

(C) The cells harboring Rif1 (wt or *rif1*PP1bsmut)-expressing plasmid or vector, as indicated, were starved for thiamine for the time indicated. The whole cell extracts were prepared and were run on SDS-PAGE containing MBP (Myelin Basic Protein) in the gel. In-gel kinase assays were conducted as described in "Materials and Methods". HU, treated with 2 mM HU for the time indicated as a positive control of Cds1 activation.

(D) Quantification of the results in (C).

Figure 4. Rif1 overexpression induces unequal chromosome segregation and DNA damages.

(A) Chromosomes are visualized by *hht2* (histone H3 h3.2)-GFP (right) and the chromosome segregation was assessed in Rif1-overexpressing yeast cells (KYP1776). Cells with unequally segregated chromosomes (indicated by mazenta arrowheads) or entangled chromosomes (indicated by blue arrowheads) increased at 24 hr after Rif1 overexpression (left).

(B) Rif1 was overexpressed in cells expressing Rad52-EGFP by depletion of thiamine for 24, 48 and 72 hr. Rad52-EGFP foci in the cells were observed under fluorescent microscopy (KYP1777, KYP1778, KYP1860 and KYP1861). The numbers of Rad52 foci (representing DNA damages) were counted, and cells containing 0, 1, 2 or >3 foci were quantified. The extent of DNA damages increased with the duration of Rif1 overexpression.

Figure 5. Cells with short tubulin spindles are accumulated in Rif1-overexpressing cells in a manner dependent on spindle assembly checkpoint (SAC)

(A) Rif1 was overexpressed in cells expressing *GFP-α2tub* and cells with short or long spindle microtubules were counted (KYP1779 and KYP1780). In the upper panels, the photos of cells with short mitotic spindles and those with long spindles are shown.

(B) Rif1 was overexpressed in the spindle assembly checkpoint activation mutants, *mad2*Δ or *bub1*Δ, and cells with spindle microtubules were counted (KYP1815, KYP1816, KYP1817 and KYP1818).

(C) SAC is induced in Rif1-overproducing cells. Cells expressing Sad1-GFP (spindle pole body) and Cut2-GFP (securin) were monitored under fluorescent microscope starting from the time when spindle pole bodies started to separate (t=0). Mitotic spindles between the two SPB disappear and the nuclear Cut2 signal disappear in non-overproducing cells by 14 min (KYP1836), while those in Rif1 overexpressing-cells stay as late as for 38 min (KYP1837). White arrowheads indicate Sad1. The drawing shows the nuclear signals of Cut2 (pale green) and two dots of Sad2 and connecting microtubules. The strong green signals indicating by * in Rif1wt OE samples represent a dead cell.

(D) Spot tests of SAC mutant cells overexpressing Rif1 (KYP025, KYP1805, KYP1815, KYP1816, KYP1817 and KYP1818).

(E) Fractions of cells with aberrant morphology (indicated by arrowheads) are scored in the wild-type, *mad2*Δ or *bub1*Δ cells overproducing the wild-type Rif1 (KYP025, KYP1805, KYP1815, KYP1816, KYP1817 and KYP1818). Cells with aberrant morphology include multi-septated cells, cells with misplaced septum, enlarged cells, septated dead cells, and cells with breached morphology. Left, phase contrast images of the cells; right, quantification of cells with aberrant morphology. Rif1 OE, Rif1 overexpression. In (**A**), (**B**) and (**E**), cells were grown in medium lacking thiamine for

18 hr.

Figure 6. Requirement of chromatin binding for growth inhibition and chromatin binding profile of overexpressed Rif1.

(A) Rif1 mutants were overexpressed in the wild-type (KYP1781 and KYP1782) and *hsk1-89* cells (KYP1783 and KYP1784), and spot tests were conducted. R236H mutant binds to chromatin but L848S mutant does not (Kobayashi *et al*. 2019).

(B) KYP1268 (*nda3-KM311*, Rif1-His$_6$-Flag$_{10}$; blue) and MS733 (*nda3-KM311*, nmt1-Rif1-His$_6$-Flag$_{10}$; red) were cultured in PMG medium containing 15 μM thiamine. The cells were washed with fresh PMG medium without thiamine and grown at 30°C for 12 hr. The cells were arrested at M-phase by shifting to 19.5°C for 6 hr, and then were released from M-phase by addition of an equal volume fresh PMG medium pre-warmed at 43°C. At 20 min after release, the cells were analyzed by ChIP-seq. Two known Rif1bs are indicated by arrowheads.

(C) Motif Logo of the conserved sequence motif identified by MEME suites from the sequences of the Rif1 binding segments determined by ChIP-seq in (B), and distribution of motif position probability determined by STREME (provided from MEME suites) on the 300-bp sequences centered on the Rif1-binding summits at the 128 and 169 peaks of "Rif1 no OE" and "Rif1 OE", respectively.

(D) Binding of Rif1 to Rif1bs$_{I:2663kb}$, Rif1bs$_{II:4255kb}$, Telomere associated sequences (telomere of chromosome II) and ars2004 (non-Rif1bs) was measured in the wild-type cells harboring vector, pREP41-Rif1-Flag$_3$, or pREP41-*rif1*PP1bsmut-Flag$_3$ by ChIP-qPCR. Cells were grown in the medium lacking thiamine for 18 hr before harvest. The IP efficiency was normalized by the level of input DNA.

Figure 7. Chromatin morphology of the cells after induction of Rif1 expression.

Cells expressing GFP-fused Histone H3 (h3.2-GFP) were observed under fluorescent microscope after induction of Rif1 protein for 10 hr or 18 hr, as indicated. **(A, B)** Overexpression of wild-type (KYP1776) or PP1bs mutant (KYP1842). **(C, D)** Overexpression of L848S [chromatin binding-deficient] (KYP1844) or R236H [chromatin binding-proficient] (KYP1843) mutant. **(A, C)** Phase contrast and fluorescent images of the cells are presented. **(B, D)** Fractions of the cells with

chromatin relocated at the nuclear periphery (indicated by arrowheads in (**A**) and (**C**)) are calculated and presented.

Figure 8. The endogenous Rif1 protein was relocated upon overexpression of Rif1

(A) Rif1-mKO2 cells (KYP1866 and KYP1867), in which the endogenous Rif1 was tagged with mKO2, harboring pREP41-Flag$_3$ vector (upper) or pREP41-Rif1-Flag$_3$ (lower) were grown in the absence of thiamine for 20 hr, and were extracted by Triton X-100 and DNase I and remaining endogenous Rif1-mKO2 signals (mazenta) were observed. The nuclear envelope was stained with Nup98 antibody (green).

(B, C) The numbers (**B**) and the intensities (**C**) of nuclear foci were quantified in Rif1-mKO2 cells harboring pREP41-Flag$_3$ (Vector) or pREP41-Rif1-Flag$_3$ (Rif1OE) grown as in (**A**).

Figure 9. Cellular events induced by overexpression of Rif1 in fission yeast.

Overproduction of Rif1 leads to its aberrant chromatin binding and inhibits S phase initiation and progression through its ability to recruit PPase. Excessive chromatin binding of Rif1 results in aberrant tethering of chromatin fibers to nuclear periphery, which may directly or indirectly inhibit proper progression of chromosome segregation, eventually leading to cell death. Overexpression of the wild-type Rif1 inhibits DNA replication, whereas that of PP1bs mutant Rif1 does not inhibit DNA replication but activates replication checkpoint. Rif1 overexpression induces SAC, leading to increased cell population with short spindles, which probably antagonizes induction of aberrant chromosome structures.

Figure S1. Expression levels of Rif1 and its derivatives.

(A) Western blot analyses of expression of the full-length Rif1 and its deletion/ truncation derivatives expressed on a plasmid after transfer to medium lacking thiamine for 24 hr. All the proteins carry $Flag_3$ tag at the C-terminus and proteins in the whole cell extracts were detected by anti-Flag antibody. α-Tubulin protein level is shown as a loading control.

(B) Quantification of overexpressed Rif1 protein. **(B-a)** KYP1805 (harboring pREP41-Rif1-$Flag_3$, lanes 8 - 10) grown with 15 μM thiamine, KYP1827 (carrying Rif1-$Flag_3$ at the endogenous locus under its own promoter, lane 5 - 7) grown without thiamine, and KP1805 (lanes 11 - 13) grown without thiamine for 20 hr (overexpressing Rif1), were harvested and whole cell extracts were prepared. The extracts corresponding to the cell numbers indicated were applied to SDS-PAGE, blotted with anti-FLAG antibody or anti-α-Tubulin antibody. On the same gel, purified His_6-Rif1-$Flag_3$ (93-1400aa; expressed in mammalian cells and purified by anti-Flag column and nickel column) protein of the known concentrations were applied as a standard for estimation of the protein amount in the extracts. **(B-b, c)** The band intensities were quantified by FUSION FX software (Vilber Bio), and the values are presented. They were compared with the standards, and the amount of Rif1 in each sample was determined. The estimated protein amount and cell numbers were plotted and the numbers of the Rif1 molecules per cell were accurately determined. **(B-d)** The purified His_6-SpRif1-$Flag_3$ protein, used as a standard, was analyzed by SDS-PAGE along with BSA to determine the precise concentration.

Figure S2. Effects of Rif1 overproduction on cell growth in various mutants.

(A) Spot tests of the wild-type (WT) (KYP1785 and KYP1786), *rif1*Δ (KYP1787 and KYP1788) or Rif1-overproducing (Pnmt1-*rif1*) (KYP1789 and KYP1790) cells harboring vector (pREP42) or Hsk1+Dfp1/Him1 overproducing plasmid.

(B) Spot tests of the wild-type (WT) (KYP025, KYP015) and replication checkpoint mutant cells harboring vector (Vec) (KYP1875, KYP1877, KYP1879, KYP1881, KYP1883 and KYP1885) or Rif1-overproducing (Rif1) plasmid (KYP1876, KYP1878, KYP1880, KYP1882, KYP1884 and KYP1886). (**C**) Spots test of the wild-type (WT) and various mutant cells harboring vector (Vec) (KYP1887, KYP1889 and KYP1891) or Rif1-overproducing (Rif1) plasmid (KYP1888, KYP1890 and KYP1892). Proteins

are overproduced on plates lacking thiamine (-Thi). Plates were incubated as indicated and photos were taken.

Figure S3. Cells with aberrant microtubules increase upon overproduction of Rif1.
(A) Rif1 wt (KYP1780) or PP1bs mutant (KYP1847) was overexpressed in cells expressing *GFP-α2tub* and cells with aberrant microtubule spindles were counted.
(B) The photos of cells with aberrant microtubule spindles are shown (indicated by arrowheads). In **A** and **B**, cells were grown in medium lacking thiamine for 18 hr.

Figure S4. Sizes of nucleoli are not affected by overexpression of Rif1.
(A) Rif1 wt (pREP41-Rif1-Flag$_3$) (KYP1864) or PP1bs mutant (pREP41-*rif1*PP1bsmut-Flag$_3$) (KYP1865) was overexpressed in cells expressing Gar2-mCherry (a marker for nucleoli) and the sizes of nucleoli were measured. pREP41-Flag$_3$ represents the vector control.
(B) The graph shows quantification of the data in **(A)**. Y-axis shows the sizes of nucleoli, as measured by those of mCherry signals (diameter).

Figure S5. Evaluation of functions of Rif1-mKO2 fusion and its images in the cells.
(A) Schematic drawing of Rif1-mKO2 fusions. mKO2 polypeptide was inserted at aa1090/1091 (MIC2-11) or at aa1128/1129, which is shown as a red box (not to the actual size).
(B) Cells with indicated genotypes were serially diluted and spotted on EMM plates, and incubated at the indicated temperatures, as shown (YM71, MIC2-11, MS104, MS744 and HM214). Growth of *hsk1-89*(ts) at 30°C is not complemented by the Rif1-mKO2 fusions, suggesting they are functional.
(C) Cellular DNA isolated from the strains shown were digested by *Eco*RI and probed by telomere-specific ^{32}P-labebed DNA. Telomere function is normal in Rif1-mKO2 cells.
(D) Enlarged images of Rif1-mKO2 (red) and Taz1-EGFP (green) (MIC20-42) taken from Movies 1~3. The cells indicated by arrows are focused in movie 5. In addition to several large Rif1-mKO2 foci that colocalize with Taz1, fine and dynamically moving Rif1-mKO2 foci, that are likely to represent Rif1 on chromosome arms, can be detected in nuclei.

(E) Rif1-mKO2 signals (mazenta) in cells expressing Cut11-GFP (green). Cut11-GFP shows nuclear membrane. Upper panels, cells harboring a vector (KYP1866); middle panels, cells overexpressing wild-type Rif1 (pREP41-Rif1-Flag$_3$) (KYP1867); lower panels, cells overexpressing PP1bs mutant Rif1 (pREP41-*rif1*PP1bs mut-Flag$_3$) (KYP1868). Images were captured by KEYENCE BZ-X700 microscopy. Strong telomere signals of endogenous Rif1-mKO2 are detected in vector control cells, whereas the Rif1-mKO2 signals are diffused in the nuclei, upon overproduction of Rif1, reflecting relocation of the endogenous Rif1-mKO2 at telomere to chromosome arms by overexpressed Rif1.

Figure S6. Effects of Rif1 overexpression on nuclear signals of the endogenous Rif1 protein tagged with mKO2 (Rif1-mKO2) after pretreatment with detergent and DNase.

Rif1-mKO2 cells harboring vector (**A** and left panel of **C**) (KYP1866) or Rif1-overexpressing plasmid (**B** and right panel of **C**) (KYP1867) were pretreated with Triton X-100 and DNase I, and stained with anti-Nup98 antibody (green; nuclear membrane) and Hoechst®33342 (blue; nuclei). The Hoechst signal is very low due to prior treatment with DNase I. In **A** and **B**, mKO2 signals are in red, while they are in black in **C**. Strong telomere signals of Rif1-mKO2 are detected in vector control, while multiple nuclear foci are detected upon overexpression of Rif1. This reflects its hetero-oligomerization with the overexpressed Rif1 protein and binding to chromosome arms.

Supplementary movies

Movie1_Rif1mKO2_related_with_Fig S5D

Movie2_Taz1GFP_related_with_Fig S5D

Movie3_Merged_Rif1_Taz1_related_with_Fig S5D

Movie4_3D_Marged_Rif1_Taz1_related_with_Fig S5D

Movie5_Trimmed_Movie3_related_with_Fig S5D

Cells expressing Rif1-mKO2 (red) and Taz1-EGFP (green) at the endogenous loci were analyzed under spinning disk microscope. Images were taken at every 2 min for 2 hr as described in "Materials and Methods". The video presented is after deconvolution. Movie 1 (Rif1-mKO2, red), movie 2 (Taz1-EGFP, green), and movie3 (red+green) are the maximum intensity projection of 3D image data in 2D space. Movie 4 is a 3D image reconstruction of an earliest time point in movies 1~3. Movie 5 is an enlarged version of movie 3, focusing on the cell indicated in **Fig S5D**.

Kanoh *et al.* Figure 1

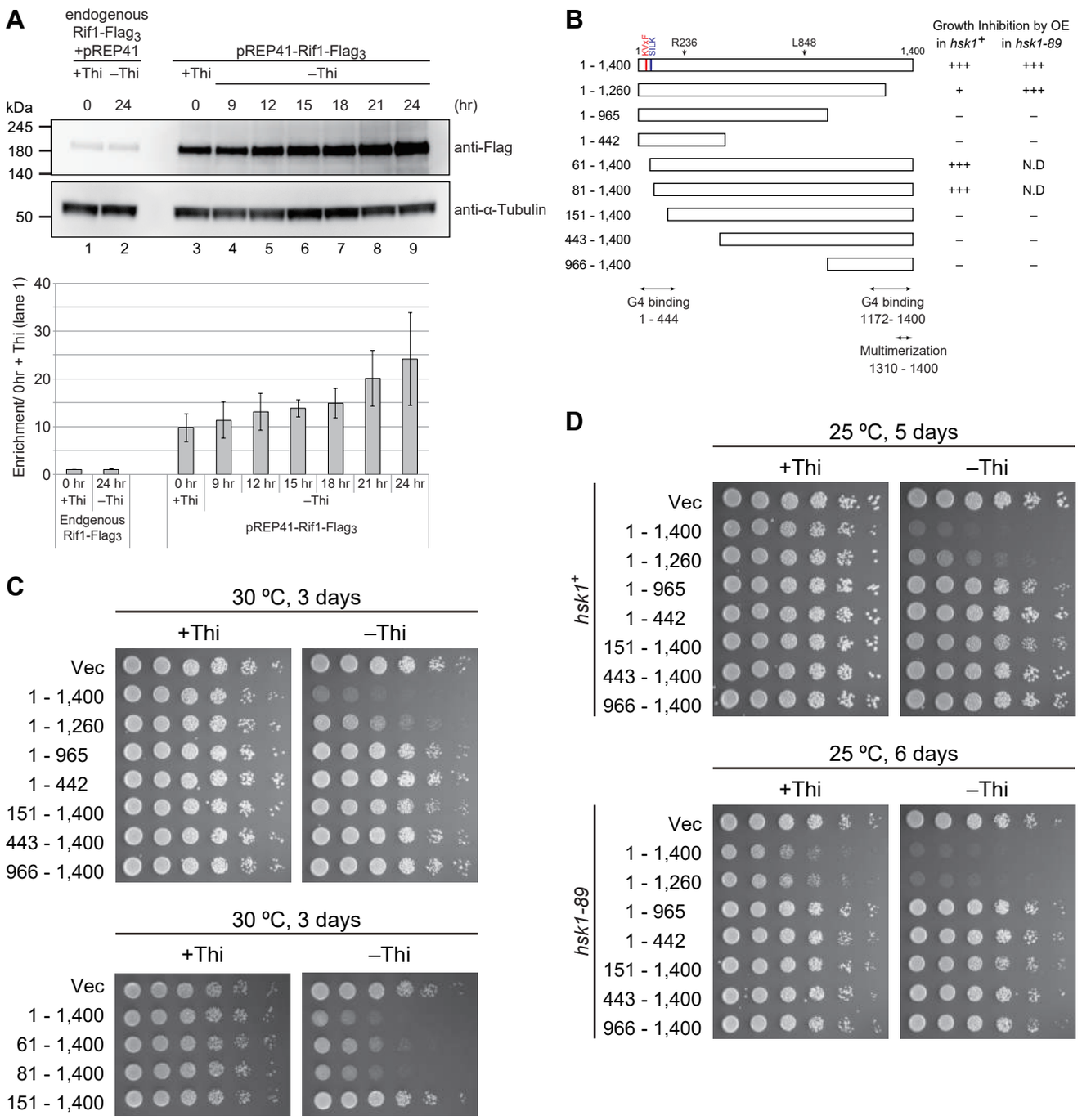

Kanoh *et al.* Figure 2

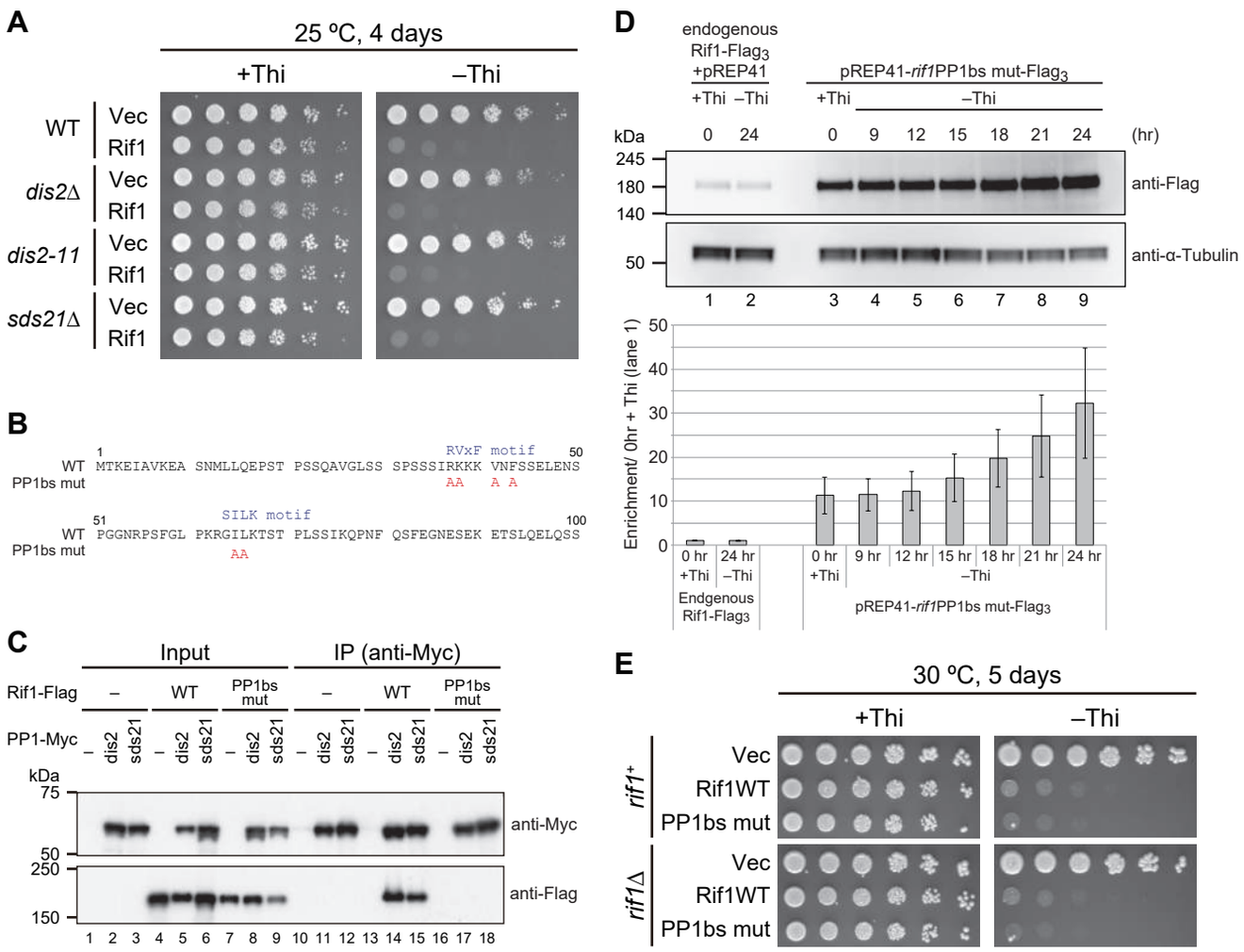

Kanoh *et al.* Figure 3

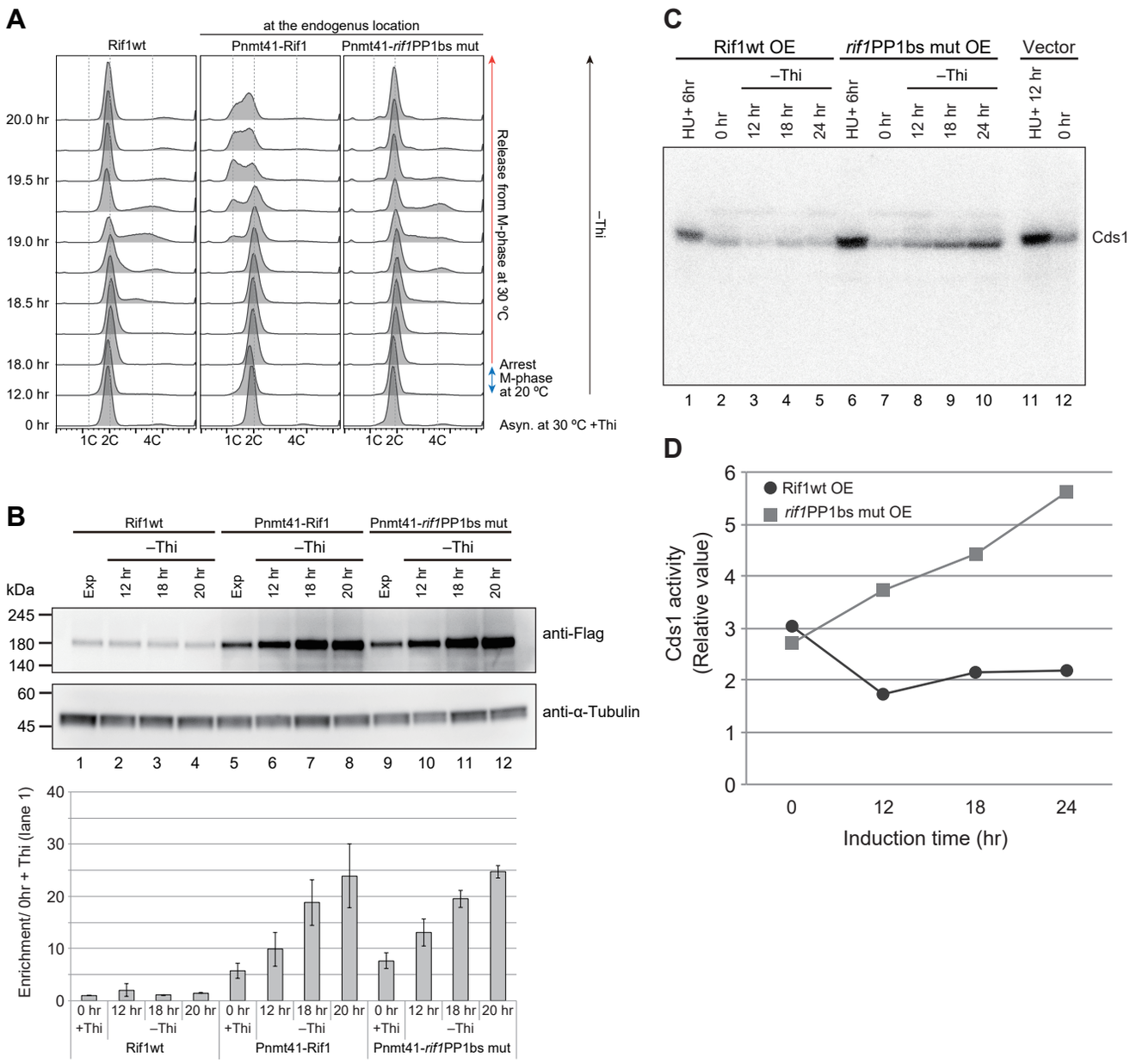

Kanoh *et al.* Figure 4

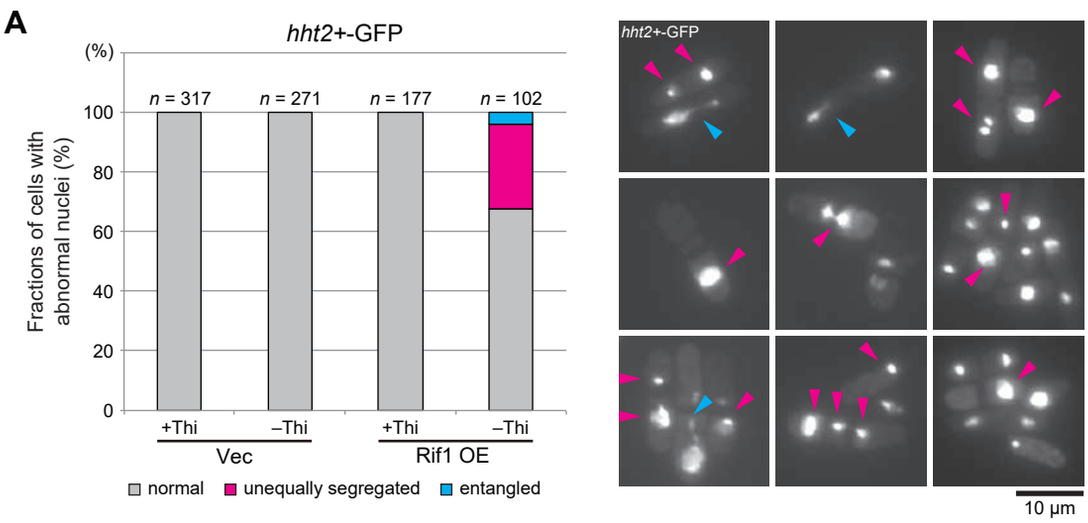

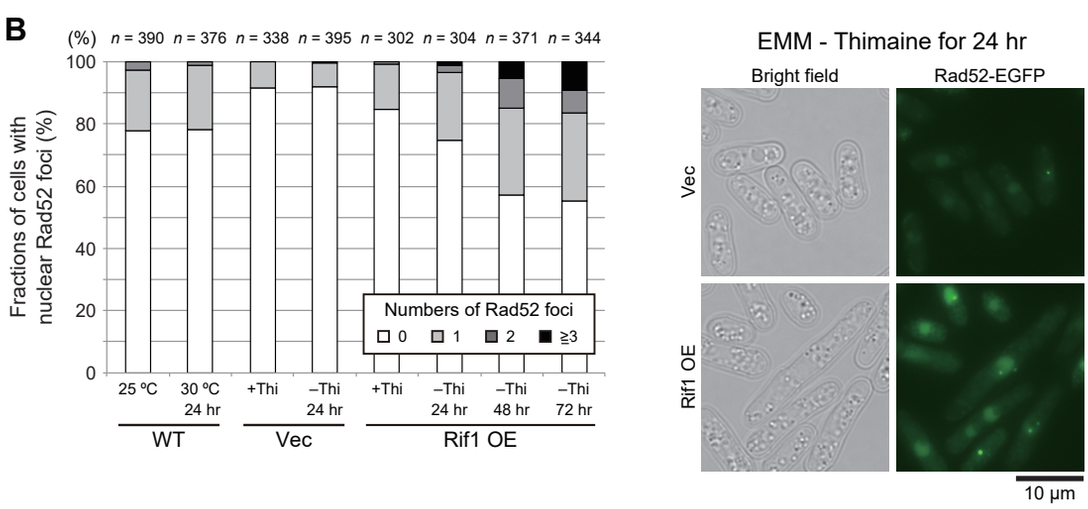

Kanoh *et al.* Figure 5

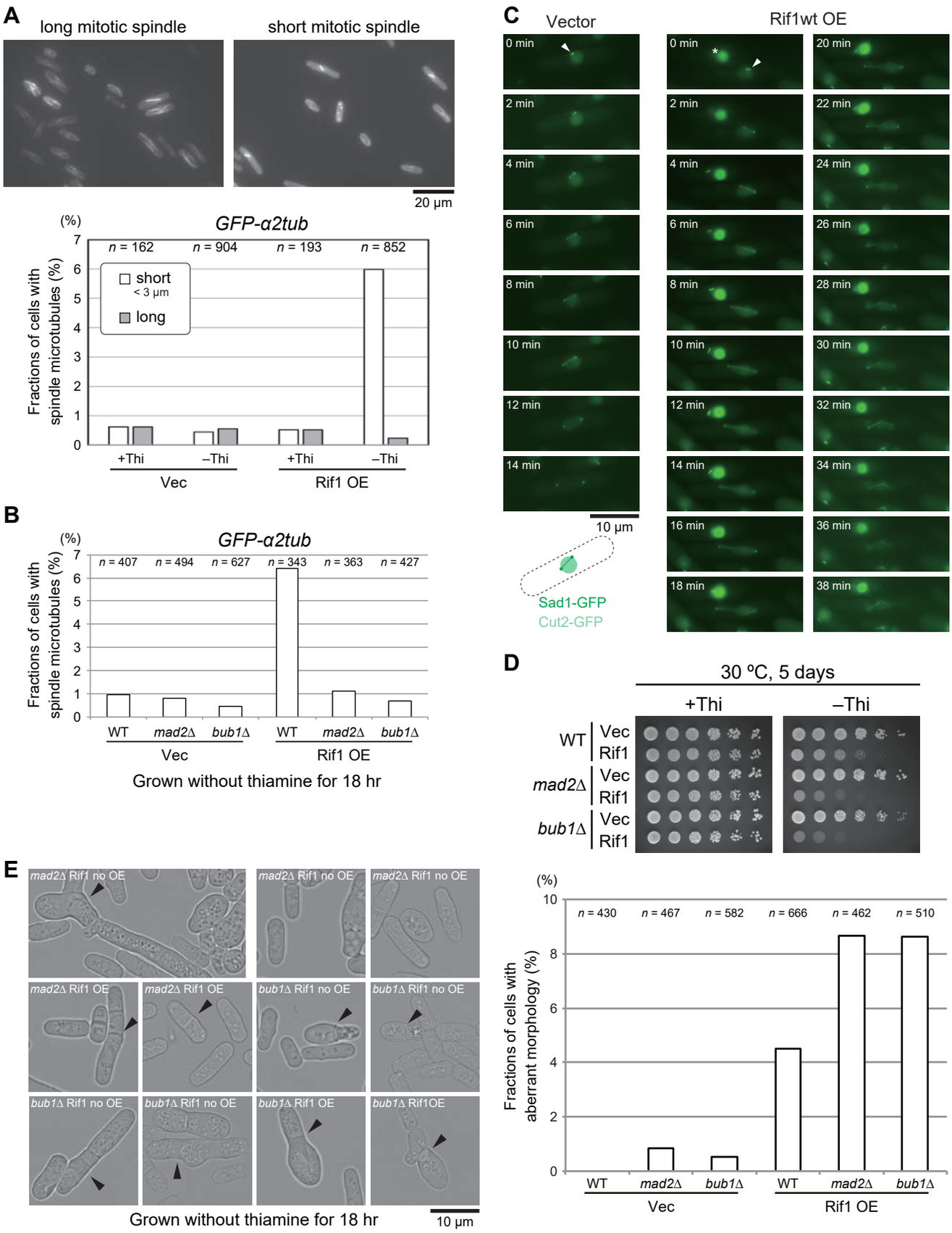

Kanoh *et al.* Figure 6

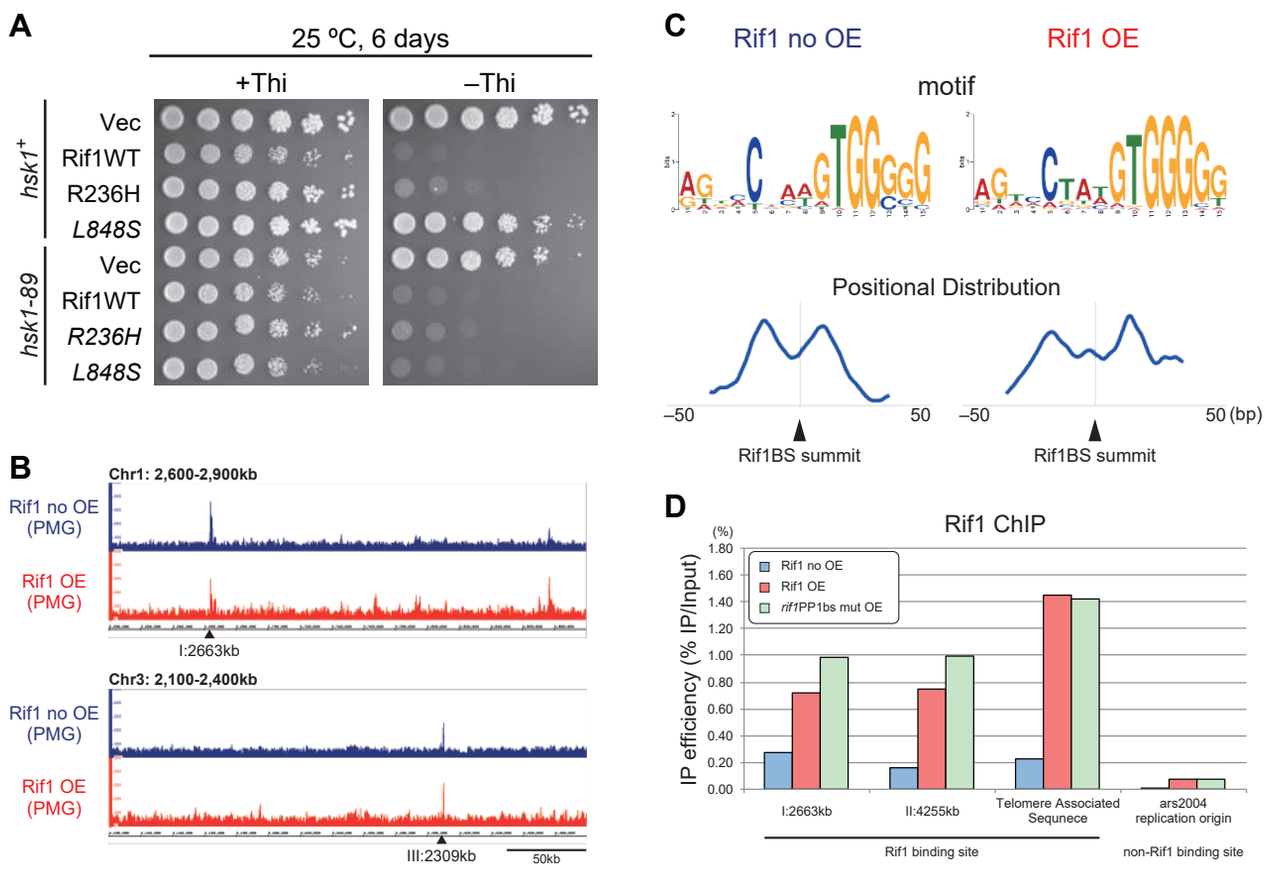

Kanoh *et al.* Figure 7

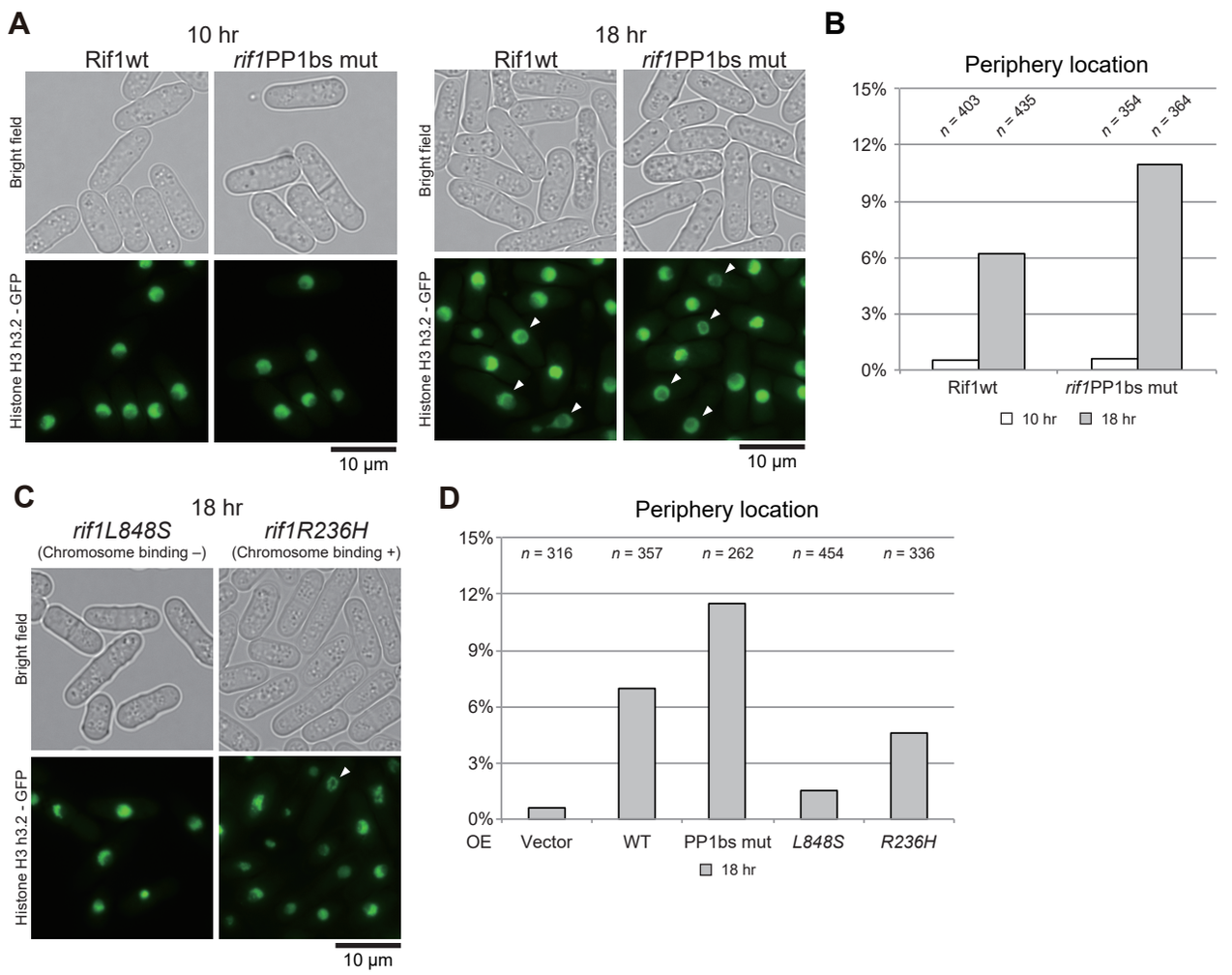

Kanoh *et al.* Figure 8

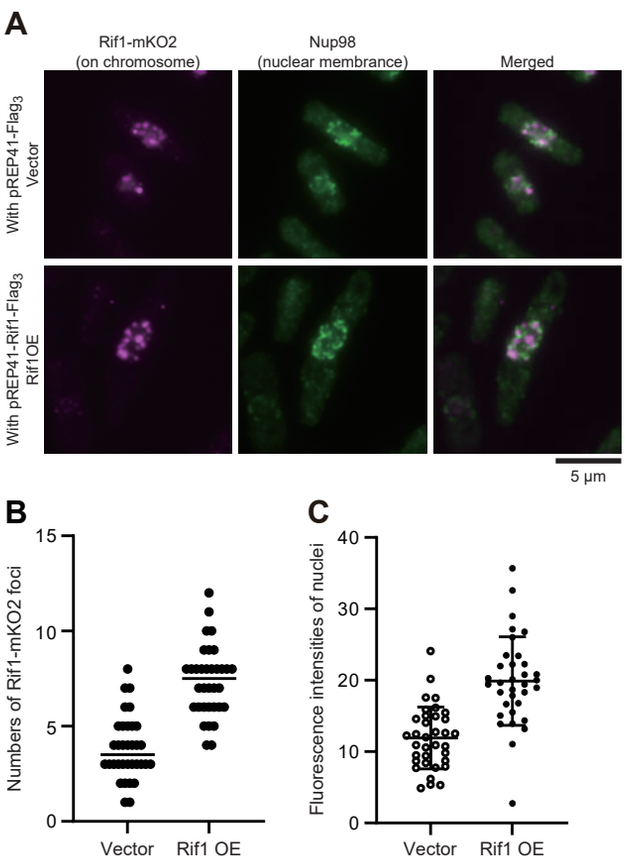

Kanoh *et al.* Figure 9

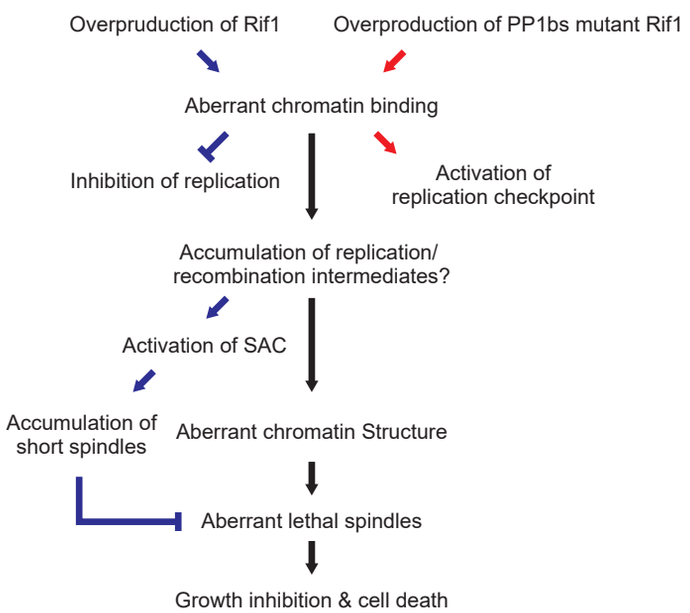

Kanoh *et al.* Supplementary Figure 1

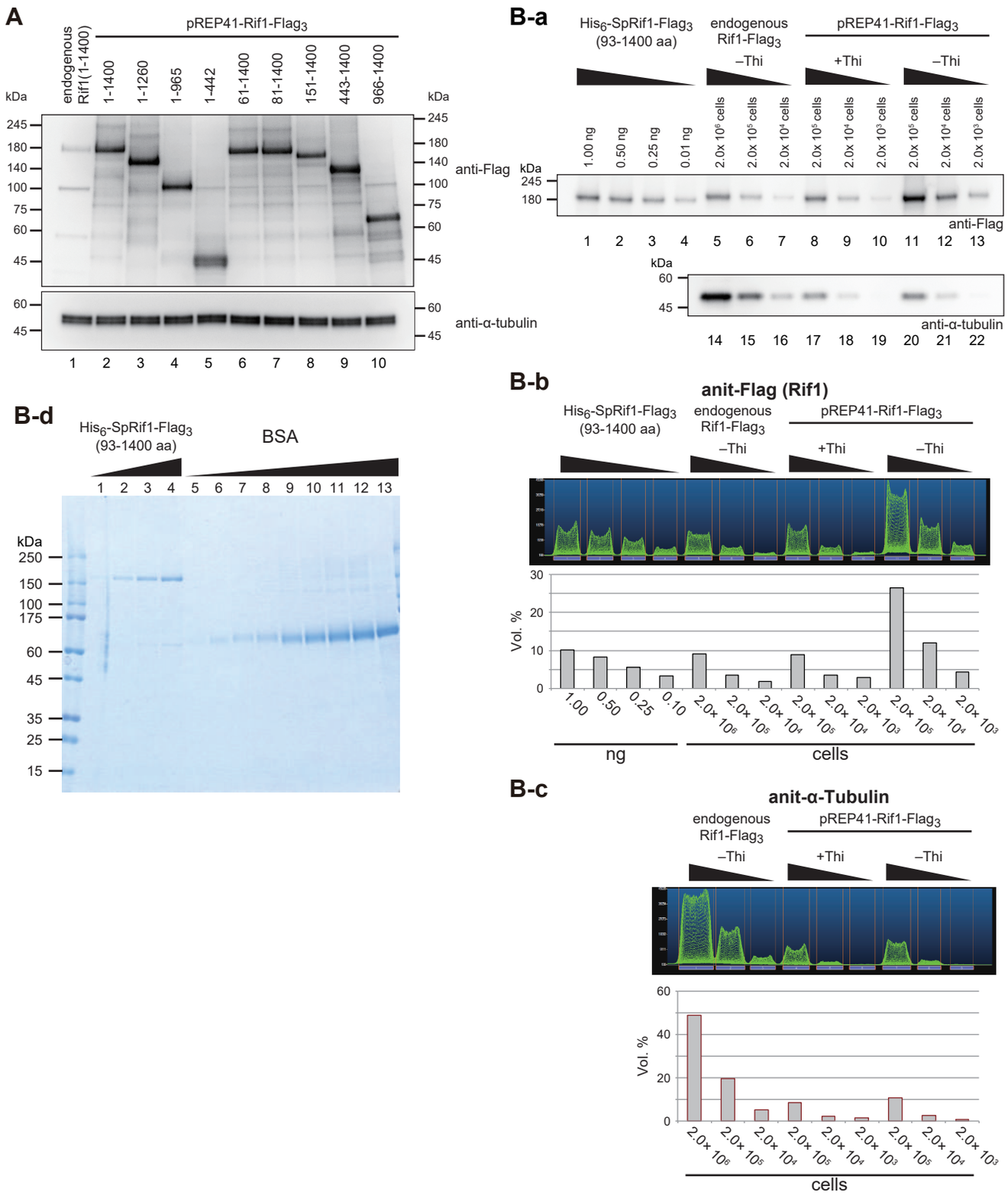

Kanoh *et al.* Supplementary Figure 2

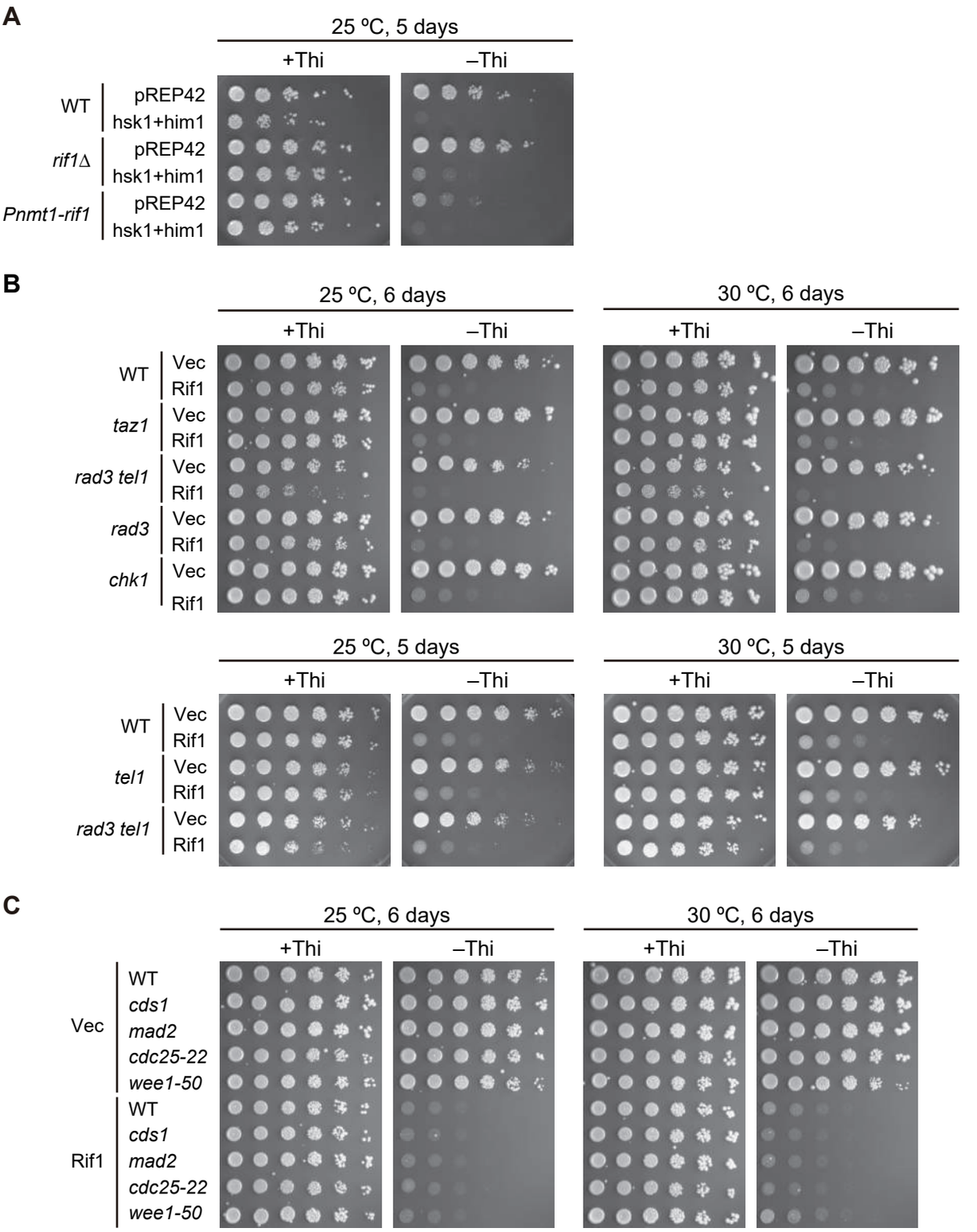

Mad2 :mitotic spindle checkpoint protein

Cds1: replication checkpoint kinase

Cdc25: M phase inducer tyrosine phosphatase

Wee1: M phase inhibitor protein kinase

Kanoh *et al.* Supplementary Figure 3

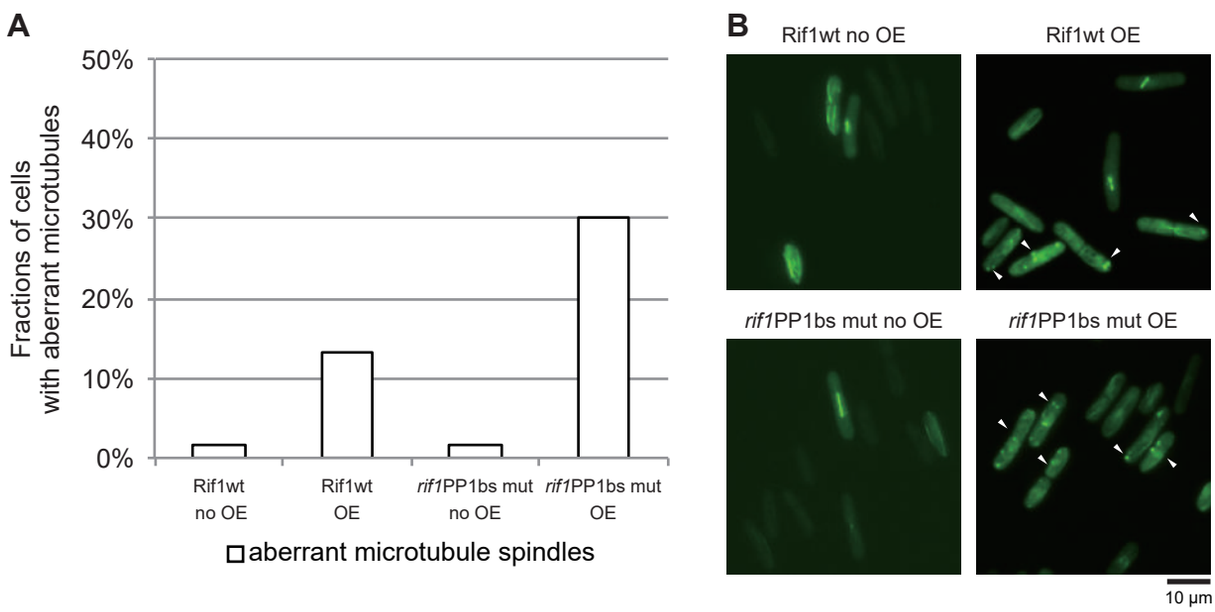

Kanoh *et al.* Supplementary Figure 4

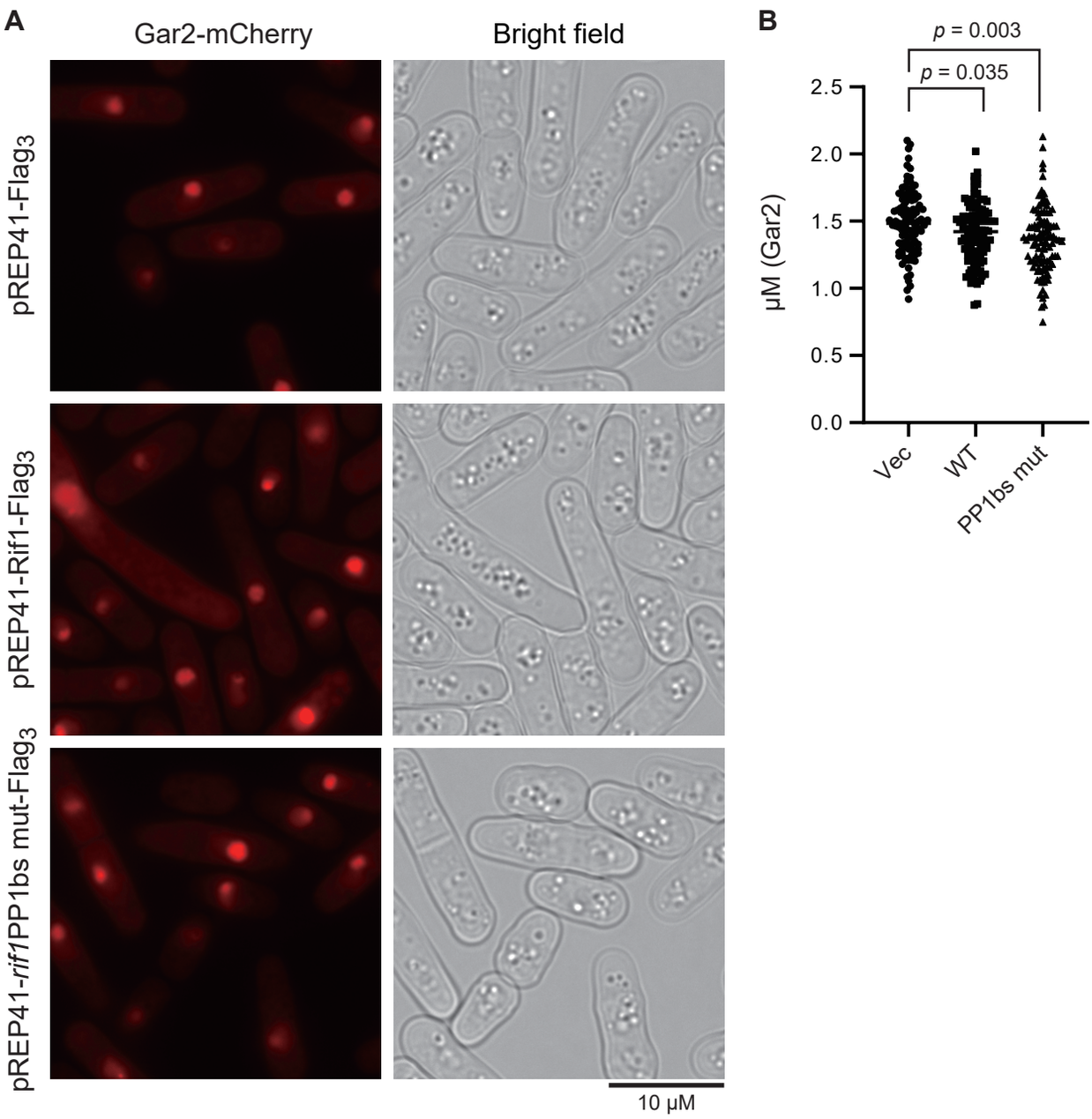

Kanoh *et al.* Supplementary Figure 5

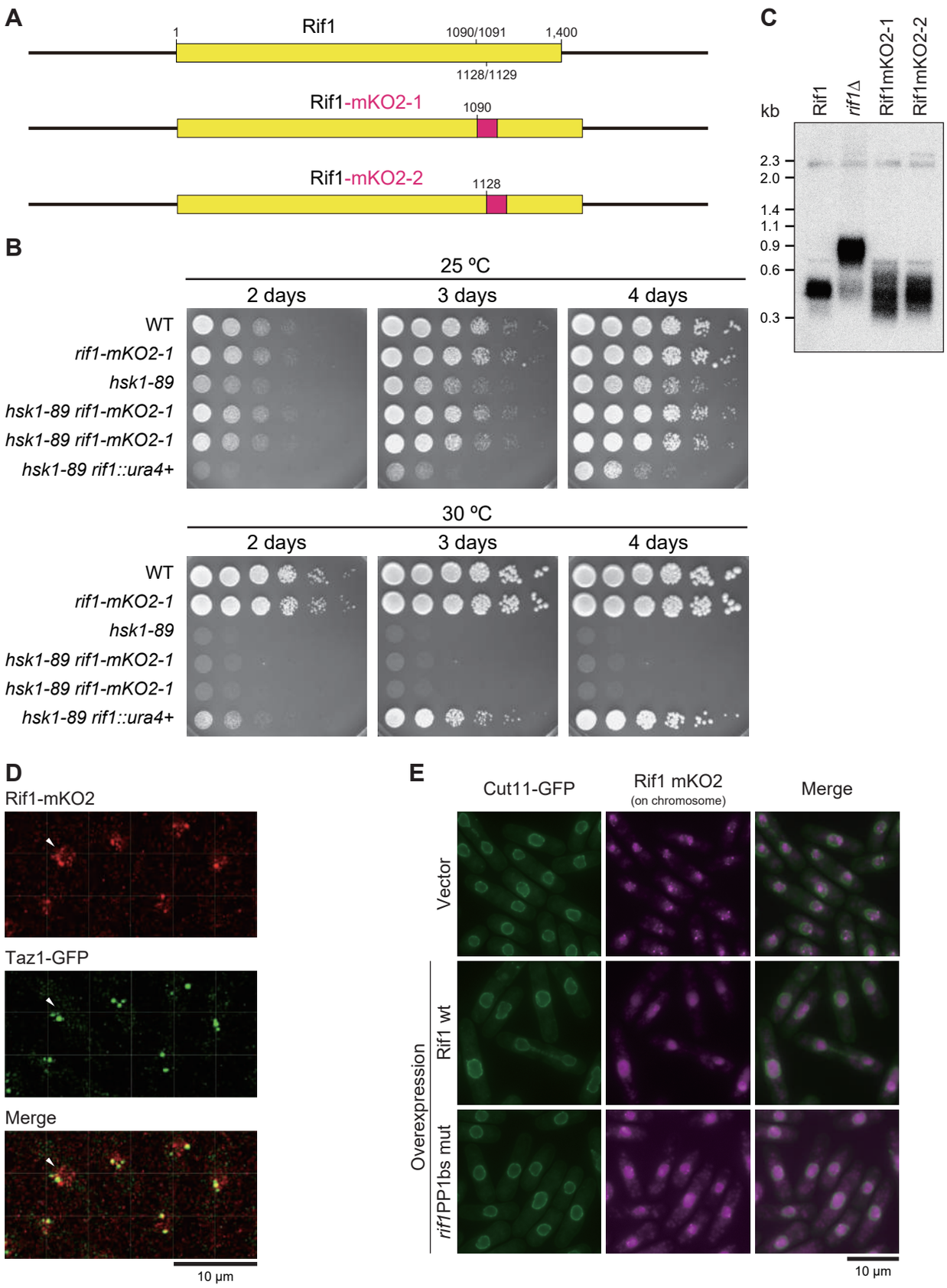

Kanoh *et al.* Supplementary Figure 6

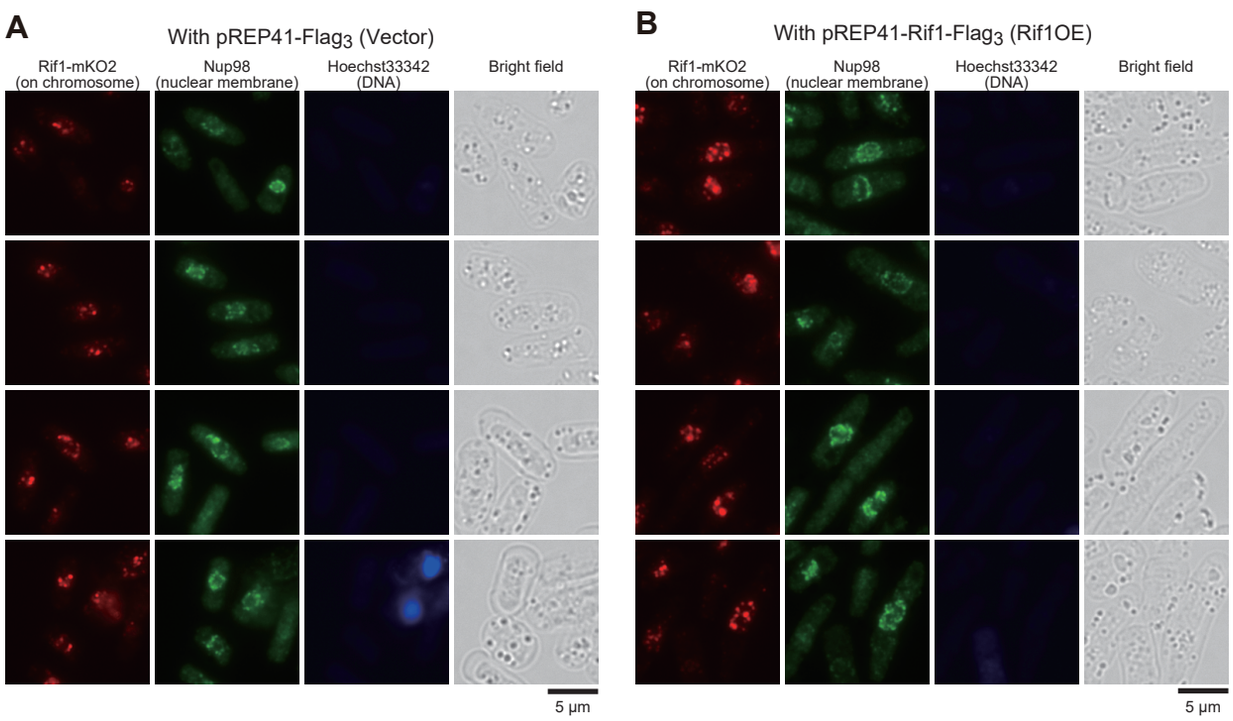

Grown without thiamine for 20 hr; pretreated with detergent and DNaseI

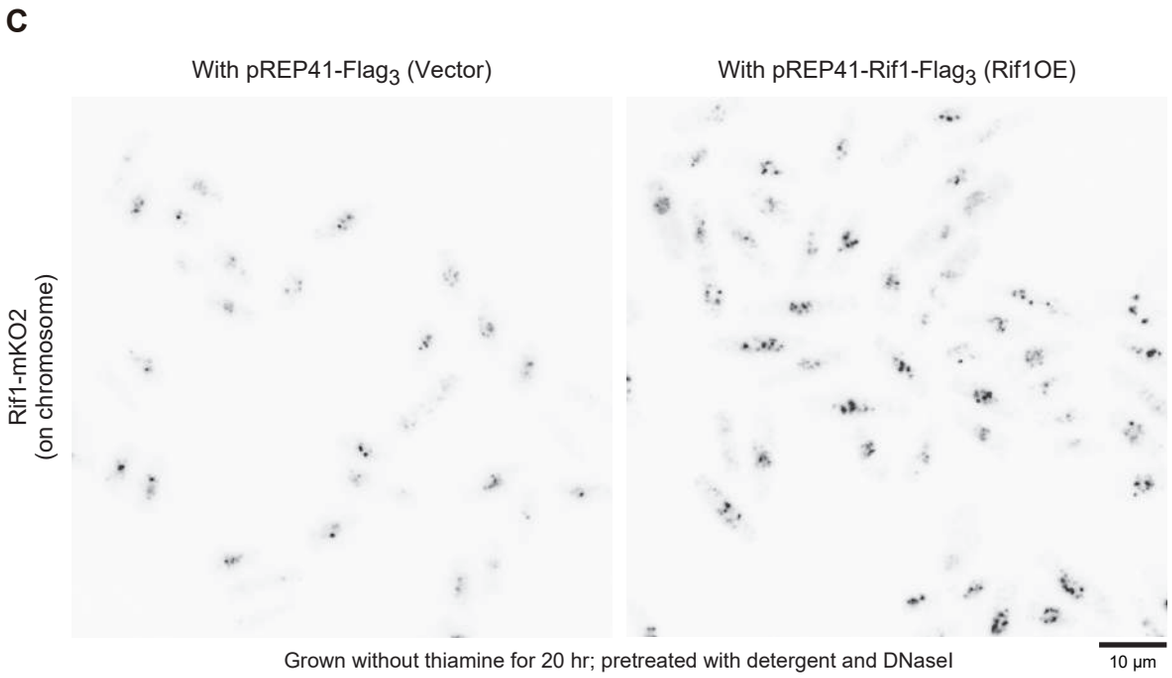

Grown without thiamine for 20 hr; pretreated with detergent and DNaseI